#731

ORTHO-/PARAHYDROGEN CONVERSION AND HYDROGEN-DEUTERIUM EQUILIBRATION OVER CARBON SURFACES

Yuichi Ishikawa,* L. G. Austin, D. E. Brown,†
and Philip L. Walker, Jr.

Department of Material Sciences
The Pennsylvania State University
University Park, Pennsylvania

*Current affiliation: Mechanical Engineering Research Laboratory, Adachi Ku, Tokyo, Japan.

†Current affiliation: B. P. Research Centre, Sunbury-on-Thames, Middlesex, England.

I. INTRODUCTION

Comparisons of the ortho-/parahydrogen transition (o-p transition) and the $H_2/D_2/HD$ equilibrium have been valuable tools in studying the rates and mechanisms of the interaction of molecular hydrogen with surfaces. Further, data on relative rates of these processes have been useful in the characterization of solid surfaces as their nature changes with heat treatment, radiation damage, and deliberate or nondeliberate contamination with impurities.

The o-p transition can be accomplished via dissociation of the hydrogen molecule followed by recombination of the atoms; this is called the "chemical mechanism." In addition, interaction of the magnetic field associated with the spin of the hydrogen nuclei with an external, inhomogeneous magnetic field causes reversal of one of the spins, which is equivalent to the o-p transition; this is called the "paramagnetic mechanism." On the other hand, $H_2/D_2/HD$ equilibration is produced by a surface only via dissociation of the molecules, so the equilibration is catalyzed only by the chemical mechanism. By comparing the rates of o-p transition and $H_2/D_2/HD$ equilibration, it is therefore possible to determine whether adsorbing surface sites are capable of chemisorption and dissociation (chemical mechanism) or operate via molecular adsorption, for in the latter case o-p transition occurs but $H_2/D_2/HD$ equilibration does not.

In this chapter, leading theories for the paramagnetic and chemical mechanisms are first considered, and prior studies on the conversion and equilibration reactions over carbon surfaces are reviewed. Then, our present and unpublished studies on these reactions over diamond and graphitized carbon black surfaces are considered in detail. It is clearly shown by our studies that the activity of carbon for the conversion and equilibration reactions strongly depends on the nature of carbon bonding (tetrahedral or trigonal) and the temperature and atmosphere which the carbon has seen. These reactions are shown to be useful for the characterization of carbon surfaces.

II. LITERATURE REVIEW

Studies on ortho-/parahydrogen conversion and $H_2/D_2/HD$ equilibration have been reviewed by Farkas up to 1935 [1], by Eley up to 1948 [2], by Trapnell up to 1952 [3], by Brennan up to 1961 [4] and, most recently, by Schmauch and

Singleton up to 1963 [5]. Only some of the main references pertinent to this chapter are mentioned.

Bonhoeffer and Harteck [6] found two distinct types of behavior for o-p transition: for charcoal and platinum black. Over charcoal, transition was rapid at low temperatures and decreased with increasing temperatures. Over platinum black, transition was slow at low temperatures, but increased with increasing temperature. Taylor [7] explained that for charcoal, transition occurred by interaction of physically adsorbed hydrogen molecules with a inhomogeneous magnetic field in the surface. Since the amount of hydrogen physically adsorbed decreased with increasing temperature, transition also decreased with increasing temperature. For platinum black, Taylor [7] suggested that transition primarily occurred following dissociative chemisorption of hydrogen molecules on the surface. Since this process is activated, the rate of this dissociation increased with increasing temperature, and, thus, the o-p transition also increased with increasing temperature.

From the effect of oxygen adsorption on charcoal on the o-p transition, Rummel [8] showed that the heterogeneous conversion at low temperatures is analogous to the homogeneous conversion produced by paramagnetic molecules. He also concluded that hydrogen is adsorbed on charcoal in the molecular form and that the o-p transition occurs in the adsorbed layer. In addition, Taylor and Diamond [9] demonstrated that the o-p conversion proceeds much more rapidly on catalysts with permanent magnetic moments (Cr_2O_3, Gd_2O_3, etc.) than on diamagnetic substances such as ZnO and Ag. Eley [10] and Farkas and Sandler [11] also showed that conversion takes place over paramagnetic materials. Farkas and Sachsse [12] showed that the o-p conversion occurred at room temperature in the homogeneous phase in the presence of paramagnetic molecules such as oxygen and nitric oxide. They concluded that conversion is caused by the influence of the inhomogeneous magnetic field of the paramagnetic molecule on the nuclear magnetic field of the hydrogen molecule during collision.

A. Paramagnetic Mechanism

A theoretical treatment of the o-p conversion by the paramagnetic mechanism has been developed by Wigner [13]. In his treatment, the hydrogen molecule

approaches the paramagnetic center with infinite velocity to the distance of closest approach r_s, is stationary for the duration of the collision t_s, and then withdraws with infinite velocity. By introducing a perturbing potential into the Schrödinger equation, caused by the interaction of the magnetic moment of the proton μ_p with that of the paramagnetic center μ_a during the collision, he was able to calculate the probability of the para-ortho transition, which may be expressed as

$$W_{o1} = \frac{24\pi^2 \mu_a^2 \mu_p^2 I t_s^2}{h^2 r_s^6 m} \tag{1}$$

where I is the amount of inertia of the hydrogen molecule, m is its mass, and h is Planck's constant.

The overall collision efficiency φ of the para-ortho transition is given by multiplying by a function G(T) which allows for the endothermicity of the transitions and the ortho-/parahydrogen equilibrium,

$$\varphi = W_{o1}\, G(T) \tag{2}$$

where

$$G(T) = \left[1 + \frac{n_p(T)}{n_o(T)}\right]\left[\frac{\Sigma_{J=0,1,2} J \exp(-E_j/kT)}{\Sigma_{J=0,2,4} (2J+1) \exp(-E_j/kT)}\right] \tag{3}$$

where $n_p(T)/n_o(T)$ is the ratio of the concentration of parahydrogen to that of orthohydrogen in equilibrium at temperature T, and $E_j = J(J+1)h^2/8\pi^2 I$. This equation has been used to predict the behavior of the homogeneous conversion and has also been of some use in predicting behavior in the heterogeneous conversion.

The above treatment was refined by Kalckar and Teller [14], who showed that it could be extended to the orthodeuterium conversion by considering the influence of the nuclear spins.

Leffler [15] calculated theoretically the conversion rate on the basis of the difference of proton-spin flip rates caused by a paramagnetic ion in the surface. Using a model in which the hydrogen molecule is adsorbed on the surface of the catalyst and oriented perpendicular to the surface, he concluded that the spin-lattice relaxation time of the paramagnetic ion greatly affects the conversion rate,

with ions having long relaxation times being better catalysts. However, the calculated rates were found to be much greater than those experimentally observed, and no correlation between the spin-lattice relaxation time and the rate was found. Leffler attributed this to an error in the assumption of the paramagnetic ion distribution, to the shortening of the spin-lattice relaxation time due to spin-spin interaction, and to cooperative behavior.

The conversion due to the interaction of an electric dipole moment with the electric field of a dipole gas has been considered by Kalckar and Teller [14]. They showed that this interaction would be about 10^3 times greater than the magnetic interactions and that this would give rise to a reaction rate 10^6 times greater than those observed in the catalysis by paramagnetic gases. Since such an effect would make it practically impossible to keep parahydrogen or orthodeuterium at room temperature, they concluded that this interaction could not exist. They also showed that an interaction between an electric field and an electric quadrapole is 10^{-2} times smaller than that for a magnetic dipole and that it would be necessary to take it into account when a very small rate is observed in the absence of a magnetic moment.

Ordinarily, the paramagnetic centers which are effecting the paramagnetic conversion are attributed to unpaired electrons. The possibility that the paramagnetic centers are the nuclei of the catalyst has been discounted because, other things being equal, the transition probability calculated on the basis of the Wigner theory is lower for the interaction of a hydrogen nucleus with a catalyst nucleus than for interaction with an unpaired electron by a factor of about 10^{-6}.

B. Chemical Mechanism

The chemical mechanism occurs when hydrogen bonds sufficiently strongly to the surface to lead to dissociation of the molecule. Taylor and Sherman [16] found a parallel between the capacity of metals to exhibit activated adsorption of hydrogen and their capacity to induce o-p conversion. The details of possible steps in the chemical mechanisms can be conveniently discussed in terms of the $H_2/D_2/HD$ conversion since the chemical steps for this conversion are virtually identical to those for o-p conversion. The proposed mechanisms are the following:

1. Bonhoeffer-Farkas [17, 18]. Dissociative chemisorption on two adjacent bare surface sites (S • S) to form a (possibly mobile) atomic layer; adsorbed atoms recombine to form molecules:

$$H_2 + S \cdot S \rightleftharpoons 2S[H]$$
$$D_2 + S \cdot S \rightleftharpoons 2S[D]$$
$$HD + S \cdot S \rightleftharpoons S[H] + S[D]$$

2. Mechanisms involving one strongly adsorbed atom reacting with a molecule.

(a) Rideal [19]. Chemisorbed atom reacts with a weakly adsorbed molecule:

$$H_2 + S \cdot S \rightleftharpoons 2S[H]$$
$$D_2 + S \cdot S \rightleftharpoons 2S[D]$$
$$HD + S \cdot S \rightleftharpoons S[H] + S[D]$$
$$HD + S \cdot S[H] \rightleftharpoons [HD]S \cdot S[H] \rightleftharpoons S \cdot S[D] + H_2$$
$$HD + S \cdot S[D] \rightleftharpoons [HD]S \cdot S[D] \rightleftharpoons S \cdot S[H] + D_2$$

(b) Eley-Rideal [20]. Chemisorbed atom reacts with impacting molecule, with no vacant site required:

$$H_2 + S \cdot S \rightleftharpoons 2S[H]$$
$$HD + S[H] \rightleftharpoons S[H] + H_2$$
$$\cdots$$

3. Schwab-Killmann [21]. Reaction between adjacent adsorbed molecules:

$$HD + S \cdot S \rightleftharpoons S \cdot S[HD]$$
$$HD + S \cdot S[DH] \rightleftharpoons [HD]S \cdot S[HD] \rightleftharpoons [H_2]S \cdot S[D_2] \begin{matrix} \rightleftharpoons S \cdot S[H_2] + D_2 \\ \rightleftharpoons S \cdot S[D_2] + H_2 \end{matrix}$$

A number of workers [22-25] have concluded that kinetic data alone do not allow clear-cut differentiation of the mechanisms given above, because the same rate forms can be obtained for different mechanisms.

C. Prior Studies over Carbon Surfaces

Bonhoeffer et al. [26] found that o-p conversion on sugar charcoal was by a paramagnetic mechanism at low temperatures and that conversion by a chemical

mechanism occurred at higher temperatures. Rummel [8] found that low-temperature oxygen adsorption enhanced the low-temperature conversion rate but that high-temperature oxygen adsorption poisoned it. Juza et al. [27] measured the magnetic susceptibility of charcoals covered with oxygen at various adsorption temperatures. They concluded that oxygen adsorbed at low temperatures was present in a paramagnetic form but that adsorbed at high temperatures was present in a diamagnetic form, i.e., atomic form. Gould et al. [28] found that charcoal did not catalyze the $H_2/D_2/HD$ equilibration at liquid air temperatures. Farkas and Farkas [29, 30] found that no equilibration reaction occurred at -195°C on charcoal. This again supports a paramagnetic mechanism for o-p conversion at these temperatures. However, it is not clear whether the inhomogeneous magnetic field causing the conversion arises from surface parmagnetism due to the presence of unsaturated carbon atoms or to the presence of small amounts of surface paramagnetic impurities which are probably present on charcoal.

Turkevich and Laroche [31] prepared a set of charcoals by heat treatment of glucose from 380 to 950°C. These samples were characterized by electron spin resonance (ESR) to determine the number of unpaired electrons and were used as catalysts for the conversion and equilibration reactions. It was found that the charcoal prepared at 605°C had the maximum in area (maximum number of free electrons) and the minimum in width of its ESR line. This sample also showed maximum activity for the o-p conversion at liquid nitrogen temperatures but a low activity in catalyzing the H_2-D_2 equilibration at 50°C. As the temperature of outgassing was increased from 605 to 950°C, the samples showed a decrease in their ability to catalyze the conversion at liquid nitrogen temperatures but an increase in their ability to catalyze the equilibration at 50°C. Simultaneous broadening of the ESR line with increasing heat treatment temperature indicated increasing interaction between electrons. They suggested that H_2-D_2 equilibration is not associated with the presence of individual noninteracting electrons, but rather with a pool of interacting electrons. However, Rossiter et al. [32] used a graded series of pure sugar charcoals similar to that prepared by Turkevich and Laroche and found that none of these charcoals was able to catalyze the equilibration, not only at 50°C but also up to temperatures as high as 540°C. They

concluded that pure carbon surfaces, with or without carbon-oxygen surface complexes, are incapable of catalyzing the equilibration and that the observations by Turkevich and Laroche must be the result of some catalytic impurity inadvertently incorporated into their charcoal samples.

D. The Surface of Carbon

1. Diamond

Diamond is an example of a crystal which is entirely covalent, as indicated by the open structure and the cohesive energy of the crystal. When a crystal is cleaved, the covalent bonds spanning the cleavage are ruptured, and in vacuum the surface atoms acquire free valencies.

Koutecky and Tomasek [33] and Koutecky [34] have discussed the electronic structure of diamond and attempted to relate the existence of surface states to the normal bonds of the crystal lattice. The (111) plane intersects one of the localized bonds formed by sp^3 hybrid orbitals of each surface atom, giving rise to a surface free valence as shown in Fig. 1. The (001) plane cuts through two bonds of each surface carbon atom in the crystal. However, in this case, the interaction between these two free sp^3 hybrids probably produces rehybridization of the hybrid orbitals. They concluded that while the (111) surface is characterized by a polyradical, the (100) surface is characterized by lone electron pairs which tend to form donor-acceptor bonds with gas molecules.

Pugh [35] has discussed surface states on the (111) surface of diamond based

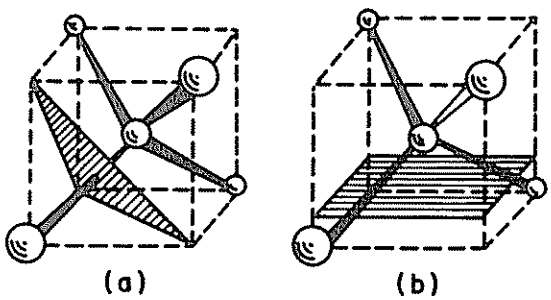

FIG. 1. Position of the $2sp^3$ orbitals of boundary atoms in diamond. Crystal bounded (a) by the (111) plane and (b) by the (100) plane.

on the linear combination of bond orbitals. He considered that the surface bonding arrangements are represented by a system of "dangling hybrids."

Low-energy electron diffraction (LEED) studies of Ge and Si suggest that the atoms on the (100) surface are displaced from their ideal positions in directions perpendicular to rows in the (110) azimuth, with the adjacent rows being displaced in opposite directions [36, 37]. However, no displacement has been observed on the (100) diamond surface [38]. Green and Seiwatz [39] have considered the energetics of surface bondings for the model proposed by Schlier and Farnsworth [36] for clean (100) surfaces of Ge and Si. From a comparison of the energy released by formation of new bonds between surface atoms with the energy required to distort the lattice into the new structure, they have concluded that little or no rearrangement should occur on the (100) diamond surface and that the surface atoms would be divalent rather than tetravalent. Further, they concluded that the electrons which were in the projecting sp^3 orbitals would form a lone pair of equal s and p character.

Marsh and Farnsworth [40] have demonstrated by LEED that the surface of clean diamond is far from ideal. Fractional-order diffraction maxima were observed, indicating a regular shifting of surface atoms from their ideal positions. Lander and Morrison [41] have also observed that the LEED pattern from the atomically clean (111) surface of diamond is characterized by extra features at half-order reciprocal lattice positions. They have proposed a warped benzene ring model to interpret their data.

The diamond which occurs in the "blue ground" of the volcanic pipe of Kimberley is hydrophobic, while diamonds which occur in sediments are hydrophilic [42]. Freshly powdered hydrophobic diamond becomes hydrophilic after treatment with calcium hypochlorite and forms stable suspensions in dilute ammonia due to the formation of surface oxides [42].

Storfer [43] investigated the chemisorption of hydrogen on diamond. He showed that no measurable amounts of hydrogen were adsorbed at either 155 or 205°C on powdered diamond which had been outgassed at 330°C for 24 hr. However, he later used diamond powders which were outgassed at 800°C [44] and found a measurable adsorption capacity. He attributed the discrepancy in these two sets of results to the oxide film which cannot be removed by outgassing at 330°C.

Barrer [45, 46] investigated the chemisorption of oxygen, hydrogen, carbon dioxide, and carbon monoxide on diamond. He showed that diamond chemisorbs hydrogen vigorously at temperatures above 400°C, with an activation energy of 13.7 to 22.4 kcal/mole. By admission of a little oxygen, a very stable oxide film is formed on diamond which poisons the surface for the chemisorption of hydrogen. Even at -78°C, a slight chemisorption of oxygen took place and, at temperatures between 244 and 370°C, carbon dioxide was liberated by interaction between oxygen and uncovered diamond surface. Barrer concluded that oxygen penetrates into diamond, but hydrogen is chemisorbed mainly on bare sites forming C-H bonds. He further concluded that diamond powder before outgassing can be regarded as being covered on internal and external surfaces by a layer of chemisorbed oxygen.

The existence of surface oxides on diamond has been demonstrated by Boehm and co-workers [42]. They observed that the heat of wetting of an oxidized diamond by water was greater than that for diamond outgassed or treated with hydrogen at 800°C. Acidic properties of the oxidized diamond surface were also observed. They suggested that carboxyl groups are probably bound to the corner and edges of the diamond crystallites.

Marsh and Farnsworth [40] observed that neither the (100) or (111) surface of diamond adsorbed oxygen readily at room temperature but that the (111) surface adsorbed oxygen more readily than the (100) surface at elevated temperatures.

Lander and Morrison [41] observed that when the clean surface was exposed to hydrogen (at 1000°C), the half-orders in LEED patterns disappeared. They proposed a structure with the "dangling bonds" of the idealized (111) structure tied to hydrogen, assuming that carbon atoms can migrate over distances of hundreds of angstroms in order to transform from a proposed "warped benzene ring" structure to the idealized diamond structure.

Boehm [47] showed that oxidation created some oxygenated chemical functional groups at the surface of diamond. He predicted the presence of some functional groups, that is, carbonyl on the (100) surface and ether on the (111) and (110) surfaces. He concluded that under normal conditions there are always some surface oxides at the surface of the diamond and that a pure and almost clean surface of diamond can be obtained and conserved only in high vacuum.

Sappok and Boehm [48] studied chemisorption of hydrogen, fluorine, chlorine, bromine, and oxygen on the surface of diamond powder. In addition, they employed heat of wetting, ESR measurements, and infrared (IR) spectroscopy. They showed that diamond with chemisorbed oxygen is hydrophilic, whereas diamond outgassed at 950°C or treated with hydrogen or halogens is hydrophobic. The quantity of free radicals in the surface of diamond after outgassing at 590°C was approximately 1% of the number of dangling bonds estimated from the number of surface atoms. Electron spin resonance studies showed that spin concentration and line width decrease on formation of surface compounds. Sappok and Boehm concluded that most of the unpaired spins were situated in the surface and that a considerable distortion of the crystal structure in the surface caused mutual saturation of free valencies. The IR spectra showed the presence of CH_2 groups and C-F bonds but no C-Cl bonds. The surface oxides were found to give rise to absorptions characteristic of carbonyl and ether groups.

Sappok and Boehm further extended their studies on surface oxides of diamond [49] and found that the quantity of chemisorbed oxygen increased with increasing temperature. After oxidation at 420°C, the quantity of oxygen on the surface was found to agree well with the number of dangling bonds estimated from the surface area of low-index planes, provided that most of the chemisorbed oxygen saturates two valencies of the surface. They concluded that the changes in the surface properties observed by others [40, 41] must be caused by very small quantities of oxygen sufficient only for low surface coverages.

2. Graphite

The structure of graphite is characterized by a system of infinite layers of fused hexagons. The short carbon-carbon distance (1.415 Å) within the layer planes shows that each of the three planar bonds is of one-third double-bond character [50]. All the binding energy of the fourth valence electron has been considered to be utilized entirely within the ring network as resonance energy. The layers are held parallel at a separation of 3.3538 Å (15°C) by weak van der Waals forces.

The free valencies in graphite are found at imperfections and also at the edges of the graphite layers (Fig. 2). The electronic structure of the boundary

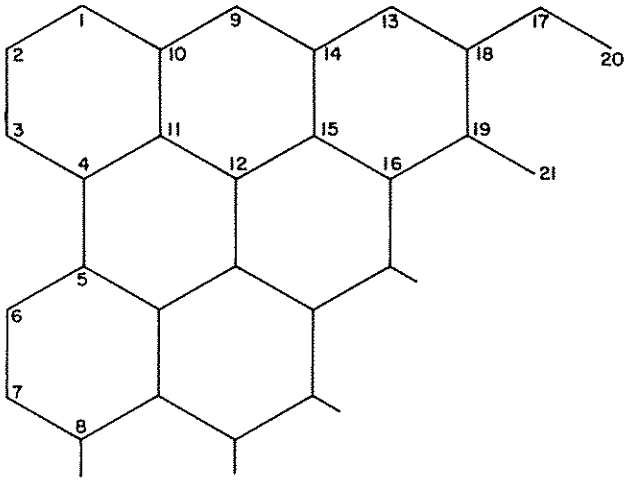

FIG. 2. Atoms in a graphite layer plane, terminated in various configurations.

atoms was discussed by Coulson [51], who proposed that there are three types of boundary situations to be considered at the edges of a graphite layer. These are as follows:

1. There are isolated unpaired electrons in sp^2 trigonal orbitals at the tails of the boundary atoms, e.g., atoms 20 or 21. Assuming that these orbitals would be noninteracting, there may be unused valence orbitals occupied by one electron, just as in a free radical. These would give rise to electron spin paramagnetism.
2. The straight edges distort, and pairs of adjacent atoms are displaced inward to form linear boundaries, e.g., atoms 2 and 3 or atoms 6 and 7. The previously described sp^2 hybrid orbitals now become $2P_x$ atomic orbitals and can be paired together effectively to form an additional bond. Thus, edge bonds may acquire a partial triple-bond character.
3. Isolated edge atoms such as 9 or 13 may revert to a divalent state s^2p^2. This would limit the resonating π electron part of the molecular layer, but would leave no unpaired electrons.

Bennett and co-workers [52] made calculations of the binding energy, binding sites, and barrier-to-surface mobility exhibited by atomic hydrogen on a graphite basal surface using extended Hückel theory and suggested that such rearrangements of type (b) proposed by Coulson [51] are energetically unfavorable.

The surface properties of graphite with reference to chemical adsorption and reactivity have been the subject of numerous papers. In adsorption studies on graphite wear dust, Savage and Brown [53] found that a small part of the surface (1 to 4%) was chemically active toward hydrogen. The confirmation of this work led Savage [54] to conclude that carbon atoms in graphite can be considered to be of three main types (see Fig. 2): (a) edge atoms which lie at the boundaries of the hexagons and which are covalently bonded to only one other carbon atom, e.g., 20 or 21; (b) edge atoms which are covalently bonded to two other carbon atoms, e.g., atoms 1 or 2; and (c) face atoms or those which lie within the hexagonal network and are covalently bonded to three other carbon atoms, e.g., atoms 11 or 12.

Smith and Polley [55] investigated the oxidation of graphitized fine thermal black and found that oxygen attack occurred preferentially at specific high-energy sites on the surface which appeared to be edge carbon atoms in the layer lattice.

From the study of the formation and decomposition of the surface oxide on artificial graphites, Bonnetain and co-workers [56] postulated very reactive dangling carbon bonds which formed upon decomposition of the stable surface oxide to explain the high initial rates of combustion after degassing.

The reaction of graphitized carbon black with oxygen at low pressure was studied by Laine and co-workers [57, 58]. They proposed a carbon surface which contained active sites on which oxygen could adsorb. These sites were thought to be carbon atoms at the edges of the graphite crystallites.

Walker [59] and Bansal et al. [60, 61] studied the chemisorption of oxygen and hydrogen on ultraclean Graphon surfaces (cleaned by heating at 1000°C in a vacuum of 10^{-9} torr). They found discontinuous straight lines in Elovich plots of their data, indicating the existence of different kinetic stages. They suggested that these definite and different kinetic stages indicate the existence of different types of sites and attributed them to different C-C spacings between surface carbon atoms on which oxygen or hydrogen could dissociatively chemisorb.

E. Electron Spin Resonance Studies on Carbons

The origin of all spin centers in carbon is still unsolved despite many years of discussion. Mrozowski [62] has shown that the ESR signal obtained from

graphitic materials can be interpreted in terms of a dual origin, that of conduction carriers and that of localized spin centers. He observed that the g value for conduction carriers is lower than the directionally averaged graphite value due to the combined effect of displacement of the Fermi level and the spreading apart of the layers occurring with insertion of ions, atoms, or molecules between the layers, both causing a change in spin-orbit interaction. The nature and origin of conduction carriers has been fairly well defined by single-crystal graphite studies [63, 64], where the results are not confused because the contribution of localized spin centers is insignificant. As to the nature and origin of the localized spin centers, it is not clear.

A number of studies have been carried out on carbons in order to determine the nature of localized spin centers. These studies have been concerned with the influence of oxygen chemisorption [65], heat treatment temperature [66], and change in surface area (by grinding) [67] on the number of spin centers. The results obtained suggest considerable modification of the surface.

Seanor [68], using the parahydrogen conversion to study the spin centers of a series of carbon chars, found that there was a maximum in the plot of the number of spin centers vs the amount of oxygen chemisorbed on the char surface. He suggested that small amounts of oxygen can form quinone structures which place restraint on the amount of delocalization allowed via the π bonding.

Such maxima, at around 600°C, have been observed by several other workers, although the explanations suggested are somewhat different (graphitization [69], release of CO_2 [70]).

Michael [71] showed that a direct relationship existed between oxygen chemisorbed on the Graphon surface and the intensity of the ESR absorption. He concluded that spins which cause the signal were localized on oxygen species chemisorbed on the edge carbons of the graphite planes and suggested the existence of semiquinone and quinone-like structures in the graphitic layer plane.

It is clear from this and other work not described that the effect of chemisorbed oxygen is very different on different carbons and may even vary for the same carbon pretreated (i.e., burn-off) in different manners. This complexity makes a complete interpretation of the ESR data extremely difficult. It would thus seem that if one is to obtain a more detailed picture of the behavior of the

oxygen-carbon system, it is important to understand how various pretreatments might change the distribution of the various surface groups which can be present.

Studies of ESR absorption and o-p conversion could yield information about unpaired electrons in surface states and how these interact with electrons in the π conduction band. They could also yield information on certain oxygen species with unpaired electrons, if these also exist in the surface. In theory, it is anticipated that ESR absorption will measure unpaired electrons in both the conduction band and surface states, whereas o-p conversion will measure only unpaired electrons in surface states. Therefore, a parallel study of ESR absorption and parahydrogen conversion should distinguish unpaired electrons in surface states from those in the conduction band.

III. THEORY

A. Paramagnetic o-p Transition

As noted in the introduction, one of the problems with analysis of these types of reactions is that different mechanisms give very similar kinetic forms. However, we shall compare a number of different mechanisms with special attention to the effect of pressure and temperature, and the plausibility of the transition states. Let us first investigate the kinetic form that is expected for the paramagnetic transition. The reactions can be written as follows:

$$p\text{-}H_2 + S \underset{k_d}{\overset{k_a}{\rightleftharpoons}} S[p\text{-}H_2]$$

$$o\text{-}H_2 + S \underset{k_d'}{\overset{k_a'}{\rightleftharpoons}} S[o\text{-}H_2]$$

$$S[p\text{-}H_2] \underset{k_b}{\overset{k_f}{\rightleftharpoons}} S[o\text{-}H_2]$$

This final step ought, perhaps, to be elaborated in terms of mobile adsorbed material reaching a position which will cause spin reversal. However, for a given surface the probability of a transition depends on the surface concentration

of [p-H_2] or [o-H_2], and other factors can be lumped into the k_f and k_b values.

Since the quantity of gas transformed is large compared to the gas existing on the surface, it can be assumed that the surface concentrations build rapidly to almost constant values and that the total pressure of hydrogen gas P_T is virtually constant,

$$P_T = P_p + P_o + P_{pe} + P_{oe} \tag{4}$$

where P_p and P_o are partial pressures of the para and ortho forms, and subscript e refers to equilibrium.

Let C_s be the surface concentration of active sites (sites per centimeter^2), with θ_p and θ_o the fraction of these sites occupied by adsorbed para and ortho forms, and $1 - \theta_p - \theta_o$ the empty sites. Assuming a simple Langmuir kinetics,

$$\begin{aligned} p \rightarrow o \text{ rate per cm}^2 &= k_a P_p (1 - \theta_p - \theta_o) C_s - k_d \theta_p C_s \\ &= k'_d \theta_o C_s - k'_a P_o (1 - \theta_p - \theta_o) C_s \\ &= k_f \theta_p C_s - k_b \theta_o C_s \end{aligned}$$

It is now assumed that the adsorption-desorption rates of orthohydrogen are virtually identical to those of parahydrogen, which makes $\theta_p + \theta_o$ a constant.

Solving for θ_o and θ_p and using Eq. (4) gives

$$-\frac{V}{A}\frac{d(P_p/RT_1)}{dt} = \frac{C_s k_a (k_f + k_b)}{(1 + K_1 P_T)(k_d + k_f + k_b)}\left(P_p - \frac{k_b}{k_f + k_b} P_T\right) \tag{5}$$

where $K_1 = k_a/k_d$ (units of pressure^{-1}), T_1 is the mean temperature of the gas in the total reactor, V is the volume of reactor, and A is the surface area of the sample. At equilibrium,

$$K_e = P_{oe}/P_{pe} \tag{6}$$

$$P_T = P_{pe}(1 + K_e) \tag{7}$$

where K_e is the equilibrium constant $(k_a k_f k'_d)/(k_d k_b k'_a)$. Hence,

$$-\frac{V}{A}\frac{d(P_p/RT_1)}{dt} = \frac{C_s k_a (k_f + k_b)}{(1 + K_1 P_T)(k_d + k_f + k_b)}\left[P_p - \frac{k_b}{k_f + k_b}\frac{k_d k_b k'_a + k_a k_f k'_d}{k_d k_b k'_a} P_{pe}\right] \tag{8}$$

Then,

$$-\frac{V}{ART_1}\frac{dP_p}{dt} = \frac{C_s k_a (k_f + k_b)}{(1 + K_1 P_T)(k_d + k_f + k_b)}(P_p - P_{pe}) \tag{9}$$

Dividing by P_T,

$$-\frac{dX_p}{dt} = \frac{ART_1}{V}\frac{C_s k_a (k_f + k_b)}{(1 + K_1 P_T)(k_d + k_f + k_b)}(X_p - X_{pe}) \tag{10}$$

Putting the units of k_a in (molecules per cubic centimeter at temperature $T_1)^{-1}$ seconds^{-1} and integrating gives a "specific rate" as follows:

$$r_s = \frac{P_T}{1 + K_1 P_T}\frac{C_s k_a (k_f + k_b)}{k_d + k_f + k_b} = k_s P_T \tag{11}$$

Here, k_s is a specific rate constant and is given by

$$k_s = \frac{k_e V}{A} = \frac{1}{1 + K_1 P_T}\frac{C_s k_a (k_f + k_b)}{k_d + k_f + k_b} \quad \text{cm/sec} \tag{12}$$

where k_e has the meaning of gas molecules reacting per gas molecule present per unit time (units of time^{-1}). As we shall see, k_e is measured experimentally. Also, then, K_e is equal to k_f/k_b, and

$$r_s = \frac{P_T}{1 + K_1 P_T}\frac{C_s k_a k_f (1 + 1/K_e)}{k_d + k_f + k_b} \tag{13}$$

Anticipating our results, we note that the dependence of k_s on P_T is that found experimentally and expressed in Eq. (50), where

$$a = \frac{C_s k_a k_f (1 + 1/K_e)(1/K_1)}{k_d + k_f + k_b} \tag{14}$$

$$b = \frac{1}{K_1} = \frac{k_d}{k_a} \tag{15}$$

$$\varphi = \frac{C_s k_a k_f / K_1}{k_d + k_f + k_b} = \frac{C_s k_f k_d}{k_d + k_f + k_b} \tag{16}$$

Two limiting cases exist. If the rate of surface transformation is very fast, $k_f + k_b \gg k_d$,

$$k_s = \frac{Vk_e}{A} = \frac{C_s k_a}{1 + K_1 P_T} = C_s k_a (1 - \theta) \tag{17}$$

If, in addition, the rate of desorption is fast so that θ is small, $K_1 \to 0$, and k_e depends on the rate of collision of molecules with active sites (pure collision mechanism). However, as will be seen, this does not give the observed dependence on pressure; instead of b being large compared to P_T it is more often small, so that $\theta \to 1$.

The other limit is for rapid adsorption-desorption compared to surface transformation, $k_d \gg k_f + k_b$,

$$k_s = \frac{Vk_e}{A} = \frac{C_s K_1 (k_f + k_b)}{1 + K_1 P_T} = \frac{C_s (k_f + k_b)\theta}{P_T} \tag{18}$$

$$\theta = k_f C_s \qquad \text{molecules/cm}^2 \cdot \text{sec} \tag{19}$$

This is perhaps a more feasible limit.

It should be noted that under these simplifying assumptions

$$\theta = \frac{P_T}{P_T + b} \qquad 1 - \theta = \frac{1}{1 + K_1 P_T} \tag{20}$$

where P_T and b are in units of molecules per cubic centimeters. When b is in units of 10^{16} molecules/cm^3 and P_T is expressed in torr,

$$\theta = \frac{P_T(3.3)(10^{16})}{P_T(3.3)(10^{16}) + b10^{16}} \tag{21}$$

$$= \frac{P_T}{P_T + (b/3.3)} \tag{22}$$

For the Langmuir case, the assumption that the adsorption-desorption behavior of p-H_2 is identical to that of o-H_2 leads to a constant value of $1 - \theta_p - \theta_o$ at constant P_T, and hence the first-order relation to P_p must follow. Somewhat more generally, this assumption can be immediately applied to the rate equation to give

$$\text{rate} = k_a P_p C_s f(1 - \theta) - k_d \theta_p C_s \tag{23}$$

$$= k_d \theta_o C_s - k_a P_o C_s f(1 - \theta) \tag{24}$$

where $f(1 - \theta)$ is some function of empty sites. Then,

$$k_a P_T f(1 - \theta) = k_d(\theta_p + \theta_o) \tag{25}$$

Providing the sum rate of desorption is independent of the relative balance of θ_p to θ_o; then, $\theta_p + \theta_o$ must be constant to satisfy Eq. (25). Then, from

$$\text{rate} = k_f \theta_p - k_b \theta_o \tag{26}$$

we obtain

$$-\frac{V}{A}\frac{d(P_p/RT_1)}{dt} = \frac{C_s k_a f(1 - \theta)(k_f + k_b)}{k_f + k_b + k_d}(P_p - P_{pe}) \tag{27}$$

Comparison with Eq. (9) shows the same rate form, but the dependence on total pressure now depends on its effect on $f(1 - \theta)$. Finally, it can be argued that the relative rates of desorption to para or ortho forms are in the ratio θ_p to θ_o, but the rate constant k_d may be a function of surface coverage if non-Langmuir kinetics apply, i.e.,

$$k_d = k_{dc} f_1(1 - \theta)$$

where k_{dc} is a corrected specific rate constant. Again, this would not alter the basic kinetic form of Eq. (27), but the dependence on temperature and P_T would include the effect on $f_1(1 - \theta)$.

B. Chemical o-p Transition and $H_2/D_2/HD$ Equilibration

Let us now consider chemical mechanisms applied to the o-p transition, where a chemical mechanism is defined as the splitting of the original molecule. Again, it will be assumed that the energetics of adsorption-desorption are such that at a constant P_T of hydrogen, the surface coverage by all forms of adsorbed hydrogen taking part in the mechanism is constant. Let us first consider the special case of high mobility and/or rates of surface transformation. For these

conditions it can be assumed that adsorbed para form θ_p comes into equilibrium with adsorbed ortho form θ_o, where at a given temperature the equilibrium ratio is set. Then, θ_o and θ_p are set values, since P_{pe} and P_{oe} are not dependent on the proportions of the starting gas mixture. Then,

$$p\text{-}H_2 + \text{surface} \underset{k_d}{\overset{k_a}{\rightleftharpoons}} \theta_p + \theta_o \underset{k_d}{\overset{k_a}{\rightleftharpoons}} o\text{-}H_2 + \text{surface}$$

Any mechanism in which the rate of adsorption is proportional to P can then be treated as follows:

$$r = P_p k_a (1 - \theta) - u \tag{28}$$

where u is the rate of parahydrogen desorption, which is constant since θ_p is constant. At equilibrium,

$$0 = P_{pe} k_a f(1 - \theta) - u \tag{29}$$

Hence,

$$r = -\frac{V}{A}\frac{d(P_p/RT_i)}{dt} = k_a f(1 - \theta)(P_p - P_{pe}) \tag{30}$$

This is of the required rate form and would be obtained for all the mechanisms enumerated in Sec. II,B, except the Eley-Rideal mechanism, which does not involve adsorption-desorption in the transition step. The function of the empty surface varies with mechanism, but it is bound to approach unity as temperature increases, so that the assumptions made lead to a prediction of constantly increasing k_e with temperature. Equation (17) is a special case of Eq. (30) for simple Langmuir adsorption.

If we now introduce the effect of a slow surface transformation or finite rate of mobility on the surface (whichever is appropriate), it is not possible to give a general treatment leading to an equation corresponding to Eq. (30); the relative values of θ_p and θ_o vary during reaction even though the total surface coverage remains constant. For example, the Bonhoeffer-Farkas mechanism written with a slow surface step is as follows:

$$\begin{array}{lll} p\text{-}H_2 + S \cdot S \underset{k_d}{\overset{k_a}{\rightleftharpoons}} [H_+]S \cdot S[H_-] & \overset{k_f}{\underset{k_b}{\rightleftharpoons}} & \\ & & S[H_\pm] \quad \text{mobile, coverage } \theta_M \\ o\text{-}H_2 + S \cdot S \underset{k_d}{\overset{k_a}{\rightleftharpoons}} [H_\pm]S \cdot S[H_\pm] & \overset{k_f}{\underset{k_b}{\rightleftharpoons}} & \end{array} \tag{31}$$

The surface rate of para to ortho can be written as

$$r = k_f \theta_p C_s - k_b \theta_m^2 C_s^2 \tag{32}$$

and the desorption velocity u is

$$u = k_d \theta_p C_s \tag{33}$$

These lead to the required rate form,

$$r = \frac{k_a f(1 - \theta)}{1 + (k_d/k_f)} (P_p - P_{pe}) \tag{34}$$

As expected, when $k_f \gg k_d$, this reduces to Eq. (30). If k_d increases faster with temperature than k_f, the value of k_e can fall at higher temperatures. Physically, this means that small θ_p, due to immediate desorption without the adsorbed atoms leaving their adsorption sites, gives a small chance of transition to the other form. The Rideal mechanism with a slow surface transformation,

$$p\text{-}H_2 + S \cdot S[H_\pm] \underset{k_d}{\overset{k_a}{\rightleftharpoons}} [H_\pm]S \cdot S[p\text{-}H_2] \tag{35}$$

$$o\text{-}H_2 + S \cdot S[H_\pm] \underset{k_d}{\overset{k_a}{\rightleftharpoons}} [H_\pm]S \cdot S[o\text{-}H_2] \tag{36}$$

$$[H_\pm]S \cdot S[p\text{-}H_2] \underset{k_b}{\overset{k_f}{\rightleftharpoons}} [H_\pm]S \cdot S[o\text{-}H_2] \tag{37}$$

leads to

$$r = -\frac{V}{A} \frac{d(P_p/RT_1)}{dt} = \frac{C_s k_a f(1 - \theta)(k_f + k_b)}{k_f + k_b + k_d} (P_p - P_{pe}) \tag{38}$$

which is identical in form to that of Eq. (27). However, it should be noted that $f(1-\theta)$ as a function of pressure and temperature would be different between the two cases because of the different mechanisms. For simple Langmuir kinetics and mobile adsorption, $f(1-\theta)$ would be proportional to the chance of a vacant site occurring next to a filled site, which is proportional to $(1-\theta)\theta$, where θ is total surface covered by [H] and [H][H$_2$]. Assuming that coverage by [H] is much greater than by [H][H$_2$], θ would be given by $P_T(1-\theta)^2 = K_{ec}\theta^2$, where K_{ec} is the equilibrium constant of adsorption of [H].

The Eley-Rideal mechanism requires no vacant site next to a filled site,

$$p\text{-}H_2 + [H] \underset{k_b}{\overset{k}{\rightleftharpoons}} [H] + o\text{-}H_2 \tag{39}$$

and, hence,

$$r = k_f P_p \theta C_s - k_b P_o \theta C_s \tag{40}$$

Using $P_{oe}/P_{pe} = k_e$ and $P_o + P_p = P_{oe} + P_{pe}$, we obtain

$$r = -\frac{V}{A}\frac{d(P_p/RT_1)}{dt} = (k_f + k_b)(\theta C_s)(P_p - P_{pe}) \tag{41}$$

Note that k_s would increase with P_T, as θ would increase. Again, this agrees with the experiment, as will be seen, but since θ tends to zero as the temperature is increased, k_e may decrease with temperature. As before, θ depends on the adsorption-desorption relation $H_2 \rightleftharpoons 2[H]$.

It is clear that replacing hydrogen by HD and considering the reaction to H_2 and D_2 would give an identical series of rate expressions, although the equilibrium pressure of HD would depend on the initial makeup of the gas mixture as well as temperature. As developed above, the rate derived is for p-o conversion, and k_f, K_e, etc., are defined in this direction. However, the process of o-p conversion would obey the same expressions but the rate would be negative. Alternatively,

$$\text{Net rate } o \rightarrow p = -\text{ net rate } p \rightarrow o = k_s P_T [X_{pe} - X_p]$$

Similarly, the net rate for $H_2 + D_2 \rightarrow 2HD$ would be

$$r(t) = k_s P_T [X_{HDe} - X_{HD}] \quad (12)$$

IV. EXPERIMENTAL

A. Apparatus

Schematics of the experimental system are given in Ishikawa [71a]. The apparatus will be described briefly. The reaction vessel, consisting of double-walled fused quartz connected through a graded seal to a Pyrex glass system, had an apparent volume of about 4000 ml calibrated by helium at room temperature. The gas storage system consisted of four 3-liter bulbs, which were connected to a gas dosing line, and two 1-liter bulbs containing helium and oxygen. The purifying system consisted of a 2-liter bulb, a palladium-silver thimble (General Electric Corp.), a vessel containing active charcoal, and a 10-liter bulb. A mass spectrometer (Consolidated Electrodynamics Corp., Type 21-611) was connected to the reaction vessel through a variable leak. It was used to measure the rate of $H_2/D_2/HD$ equilibration and the partial pressures of gaseous species desorbed from samples during outgassing. Reaction temperatures above room temperature were obtained by employing an electrically heated furnace operating off of a temperature controller. The temperature-controlling thermocouple (chromel-alumel) was placed between the outer wall of the quartz jacket and the furnace wall. Reaction temperatures were measured with a chromel-alumel thermocouple that was placed in the quartz thermocouple well on which the sample holder rested. Temperatures below room temperature were obtained using low-temperature baths.

B. Gases and Carbons Used

Oxygen (for adsorption) and helium (for calibration of the volume) were Air Products and Chemicals, Inc., research grade. An analysis supplied with the oxygen listed the major impurities as 11 ppm nitrogen, less than 5 ppm argon, and 0.76 ppm water. For helium, the major impurities were listed as 0.5 ppm oxygen and less than 5 ppm nitrogen. Pure normal hydrogen (75% ortho/25% para) and deuterium (67% ortho/33% para) were prepared by diffusing hydrogen and deuterium from a cylinder through the palladium-silver thimble heated to red

heat. Para-enriched hydrogen was prepared by adsorption on active charcoal held at liquid hydrogen temperatures. About 4 g of active charcoal (Pittsburgh Activated Carbon Co.) were outgassed at 350°C for 2 days. With the charcoal vessel immersed in liquid nitrogen, pure normal hydrogen was adsorbed onto the charcoal and, when adsorption had reached equilibrium, the liquid nitrogen was replaced by liquid hydrogen. After approximately 5 hr, the liquid hydrogen was removed and the para-enriched hydrogen (90 to 95% p-H_2) was stored in one of the 3-liter bulbs before significant backconversion could occur. Hydrogen-deuterium mixtures were adsorbed onto active charcoal, at liquid hydrogen temperatures, to facilitate mixing.

The equilibrium concentration of parahydrogen between 10 and 500 K, the specific heat of ortho- and parahydrogen, and the equilibrium constants for $H_2/D_2/HD$ equilibration were taken from Wolley and co-workers [72]. Values are summarized in Figures 3 through 5.

The diamond used was a natural diamond powder produced in West Africa. The powder was treated with hydrofluoric acid and sulfuric acid and outgassed a' 900°C. A complete description of the diamond powder has been reported by Sappok and Boehm [48], who supplied our sample. Table 1 gives a summary of the diamond powder properties. The diamond powder was treated with oxygen, hydrogen, or chlorine in the manner described by Sappok and Boehm [48, 49],

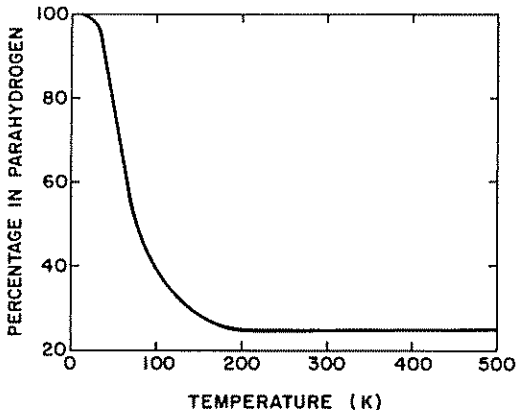

FIG. 3. Ortho-/parahydrogen composition at equilibrium.

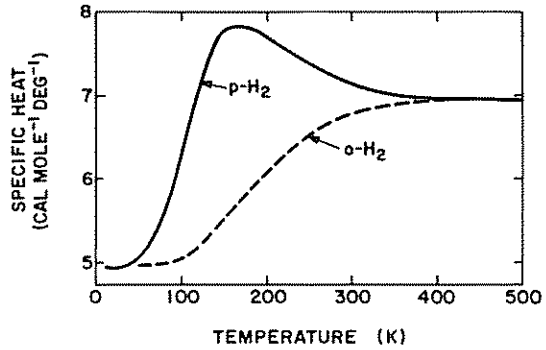

FIG. 4. Specific heat of ortho- and parahydrogen.

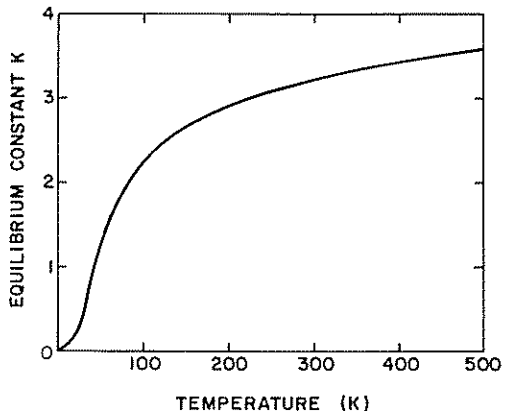

FIG. 5. The equilibrium constant for H_2-$D_2 \rightleftharpoons 2HD$.

after outgassing at 950°C. An oxidized sample was prepared by heating diamond powder in a stream of dry oxygen at 400°C for 30 min, followed by cooling in oxygen. A hydrogenated sample was prepared by heating diamond powder in a stream of hydrogen at 900°C and cooling to room temperature in hydrogen. A chlorinated sample was prepared by heating diamond powder in a stream of chlorine at 400°C for 30 min, after which the chlorine was pumped away and the sample cooled to room temperature.

The other carbon used was Graphon (Cabot Corp.), produced by the heat treatment of a carbon black, Spheron 6 (Cabot Corp.), to about 2800°C. Table 2 gives a summary of properties of Graphon.

TABLE 1
Summary of Properties of Diamond Powder

Property	Description	Method of determination
Impurities	0.2 to 0.3% Si 0.02 to 0.15% Al 0.01 to 0.02% Ca 0.01 to 0.02% Cu 0.007 to 0.01% Fe 0.006% B 0.001 to 0.004% Mg	Spectrographic analysis
Particle size and shape	0.5 μm diameter 200 Å thickness Wedge or platelet shape	Optical and electron microscopy
BET area	20 ± 2 m^2/g	

TABLE 2
Summary of Properties of Graphon

Property	Description	Method of determination
Impurities	5 ppm Ti 5 ppm Ca 1 ppm Si	Emission spectroscopy
	20 ppm S	X-ray fluorescence analysis
Particle size and shape	0.25 mm diameter agglomerate particles of chain-like structures made up of 250 Å average diameter particles	Optical and electron microscopy
BET area	76 m^2/g	

In order to obtain samples of differing activity, Graphon was oxidized at 500°C in a stream of dry air for different lengths of time up to 215 hr to obtain different amounts of burn-off. These samples were then heated at 950°C in a stream of argon and outgassed at 950°C to 10^{-8} torr. The amount of oxygen chemisorbed by the samples at 350°C at an oxygen pressure of 1 torr was measured in order to calculate active surface [58] areas. The active surface areas (ASA), calculated by assuming that every chemisorbed oxygen atom

TABLE 3

Surface Areas of Activated Graphon Samples

Burn-off (%)	BET (N_2)	ASA (O_2)	ASA (%)
0.0	76	0.2	0.3
3.7	88	1.6	1.8
15.9	99	3.9	3.9
24.9	115	5.4	4.7
37.9	128	6.7	5.2
70.5	135	7.4	5.5

occupies an area of 8.3 $\AA^2$ [58], and the BET surface areas are listed in Table 3.

C. Hydrogen Analysis

Ortho-/parahydrogen analyses were carried out by employing a micro-Pirani gauge similar in design to that used by Bolland and Melville [73]. It consisted of a fine tungsten wire (part of an electric light bulb filament of about 90 Ω room temperature resistance) spot welded to two tungsten leads, this being sealed in a uranium glass capillary. The gauge was connected to the compression limb of a McLeod gauge, which was in turn connected to the gas dosing line by a greased stopcock. In order to reduce local temperature fluctuations, the gauge was surrounded by a small metal bucket filled with mercury prior to immersion in liquid nitrogen.

The calibration of the gauge was carried out by measuring the resistance at 77, 195, 273, and 300 K with a very low bridge current to avoid heating the wire. A battery (2 V), with a 3000 Ω resistor in series, was used to provide the potential. The resistance of the wire at 170 K was interpolated from the results.

For resistivity measurements, gas samples were compressed to a pressure of 50 torr and the resistance of the wire was measured at constant potential by means of a modified Wheatstone bridge network. The maximum sensitivity of the gauge was obtained at 170 K, since at this temperature the difference in thermal

conductivity between ortho- and parahydrogen is greatest [1]. This temperature was obtained by applying 10 V to the bridge circuit, the circuit being controlled by three potentiometers (Leeds and Northrup) of 100, 10, and 1 Ω resistance. The gauge resistance was measured on a resistance box (Leeds and Northrup Co.), which could be read to 0.001 Ω by means of a galvanometer (Rubicon Instruments).

In order to analyze unknown mixtures of hydrogen, the value of the resistance at 170 K was set on the resistance box and the gauge was filled with normal hydrogen at 50 torr. In the case of parahydrogen conversion measurements above 90 K, the para-enriched hydrogen was used. The heating current was supplied by a storage battery until the wire reached the required temperature, and the potential across a 300 Ω resistance was measured. This was the working potential and was kept constant during the analysis. Then the gauge was switched off and the normal hydrogen was pumped off. The mixture was then admitted into the gauge and compressed to 50 torr, and the resistance box and heating current were alternately adjusted until the resistance remained constant at the working potential set up before the analysis. The working potential was regularly checked with normal hydrogen before the analysis.

In hydrogen-deuterium equilibration experiments, samples were taken from the reaction system and analyzed by a mass spectrometer.

D. Rate Measurements

The kinetics of the parahydrogen conversion and the $H_2/D_2/HD$ equilibration were studied as a function of pressure and temperature in a constant-volume reaction system.

The normal (or para-enriched) hydrogen or H_2-D_2 mixture was left in contact with a carbon sample for known times at known pressures. The reaction mixture was analyzed in the micro-Pirani gauge or the mass spectrometer, as described above. During rate measurements, levels of the low-temperature bath and liquid nitrogen traps were kept constant and the resistance of equilibrium hydrogen was frequently checked.

V. RESULTS

A. Over Diamond

Both the conversion and equilibration reactions were measured in the reactor in the absence of a sample at 77 and 297 K, after outgassing at room temperature or 950°C for at least 14 hr. No significant reaction was found.

It was found (Fig. 6) that the kinetic data for o-p conversion or $H_2/D_2/HD$ equilibration obeyed a first-order rate equation with respect to the concentration of para-hydrogen (or HD). That is,

$$X(t) - X(\infty) = [X(0) - X(\infty)] \exp(-k_e t) \tag{43}$$

where $X(t)$ is the molar fraction of reactant present in the gas at time t and $X(\infty)$ is the equilibrium concentration. Under some conditions, the rate of $H_2/D_2/HD$ equilibrium was almost the same as o-p conversion, indicating that a chemical mechanism was responsible for the major part of the o-p conversion rate.

Equation (43) is, of course, readily derived for a unimolecular, reversible homogeneous reaction, and k_e has the meaning of gas molecules reacting per gas

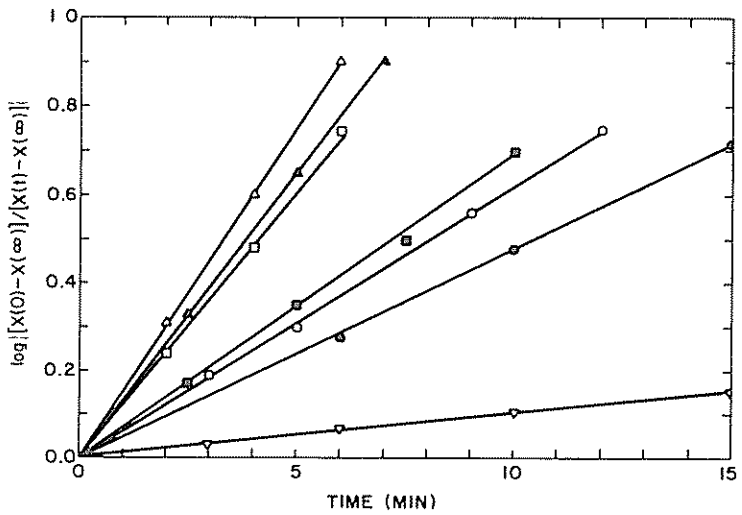

FIG. 6. Tests of first-order rate equation over diamond outgassed at 950°C; total pressure, 7 torr. Open symbols, o-H_2/p-H_2 conversion; solid symbols, $H_2/D_2/HD$ equilibration. Temperature (K): O ●, 77; △ ▲, 195; □ ■, 273; ▽, 473.

molecule present per unit time (units of time^{-1}). However, the meaning of k_e with respect to a heterogeneous reaction at constant gas volume is by no means self-evident. Equation (43) arises from the rate expression

$$-\frac{dX(t)}{dt} = k_e[X(t) - X(\infty)] \tag{44}$$

Expressing the rate of reaction in terms of molecules of gas reacting per centmeter^2

$$r(t) = -\frac{V}{A}\frac{dC(t)}{dt} \tag{45}$$

where V is the volume of reactor, A is the surface area of carbon, and C(t) is the mean concentration of reacting gas in molecules per cubic centimeter in the reactor volume. Then,

$$r(t) = -\frac{V}{A}P_T\frac{dX(t)}{dt} \tag{46}$$

and from Eq. (44),

$$r(t) = \frac{k_e P_T V}{A}[X(t) - X(\infty)] \qquad \text{molecules/cm}^2 \cdot \text{sec} \tag{47}$$

where P_T is the total gas pressure in units of molecules per cubic centimeter. (Note that, since the major part of the gas is at room temperature, conversion from pressure in torr to molecules per cubic centimeter used room temperature, not reaction temperature.) Since the use of V and A converts values of k_e to a comparable basis for all samples, we define a specific rate constant by Eq. (12), as given previously:

$$k_s = \frac{k_e V}{A} \qquad \text{cm/sec}$$

Then,

$$r(t) = k_s P_T[X(t) - X(\infty)] \tag{48}$$

Ashmead and co-workers [74] define an "absolute rate of conversion" by

$$k_m = k_s P_T \qquad \text{molecules/cm}^2 \cdot \text{sec} \tag{49}$$

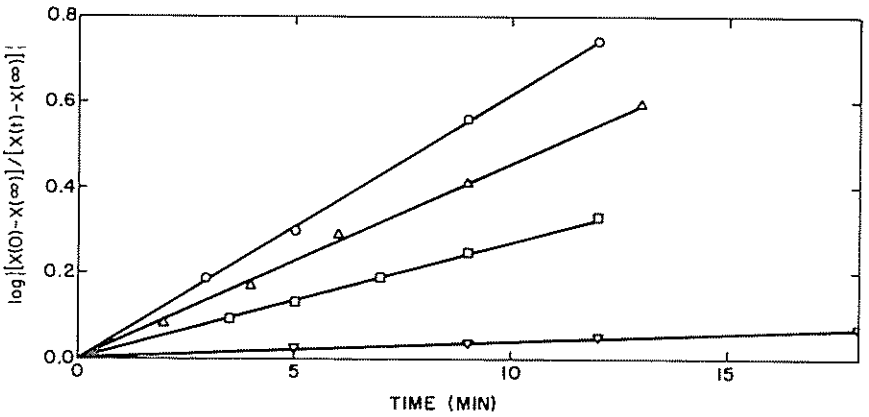

FIG. 7. Tests of first-order rate equation for o-H_2/p-H_2 conversion at 77 K over treated diamond; total pressure, 7 torr. Key: O, outgassed at 950°C; △, treated with O_2; □, treated with H_2; ▽, treated with Cl_2.

where k_m is given the physical significance of the nonalgebraic sum of the rates of o → p and p → o. To avoid using k symbolism for a rate, we use r_s for a "specific rate," defined as the rate for $X(t) - X(\infty) = 1$, as given previously in Eq. (11):

$$r_s = k_s P_T \qquad \text{molecules/cm}^2 \cdot \text{sec}$$

Figure 7 shows plots for diamond samples treated with Cl_2, H_2, and O_2, as previously described. It is apparent that the reaction still obeys Eq. (43), although the rate constant is reduced in the following order: clean, treated with O_2, H_2, Cl_2. In general, it was found that Eq. (43) was obeyed to the equilibrium point for the o-p conversion and $H_2/D_2/HD$ equilibration in the range of temperatures studies (77°K to 500°C) and for initial gas phase compositions varying from at least 25 to 95% parahydrogen.

If a true specific rate is being measured, r_s or k_s should be constant irrespective of A, when everything else is held constant. The effect of varying sample weight (or bed depth) on specific rates was studied. The sample was outgassed at 950°C before kinetic measurements were made. As the sample weight was decreased from 500 mg to 200 mg (a bed height of 0.7 cm) the specific rates of both the conversion and equilibration reactions at 77 and 195 K increased.

Further decreases in sample weight down to 10 mg produced insignificant changes in rates. The process is considered to be controlled, in part, by diffusion when more than 200 mg of sample are used. Since negligible porosity is expected within the diamond particles, the shape of the particle is presumed to be the cause of significant diffusion resistance. When the platelet-shaped particles are aligned parallel to each other, diffusion through "pores" formed by these contacts is considered to be at least in part controlling the reaction rate. All data, which will be discussed below, were obtained using approximately 180 mg of sample. Therefore, the process should not be significantly influenced by diffusion.

As discussed in Sec. III, theory suggests that the dependence of k_s on total pressure for constant V and A might be of the form

$$k_s = \frac{k_e V}{60A} = \frac{a}{P_T + b} \tag{50}$$

or

$$\frac{60A}{V}\frac{1}{k_e} = \frac{1}{k_s} = \frac{P_T}{a} + \frac{b}{a} \tag{51}$$

Thus, a plot of $1/k_e$ at constant V and A vs P_T should give a straight line. Figures 8 and 9 show the results with a diamond sample outgassed at 950°C for reaction at various temperatures. Similar plots were obtained for the samples treated with Cl_2, H_2, and O_2, and outgassed at various temperatures. It is concluded that the results agree with the form of Eq. (51), at least as a reasonable approximation. The values of a and b are given in Table 4. It will be noted that the slopes, and hence a, can be measured with reasonable accuracy but that the values of b cannot be measured accurately at low temperatures. The value of a is a new rate parameter which summarizes values of k_s over a range of pressures. If P_T is converted to units of molecules per cubic centimeter, a is in units of molecules per centimeter^2 · seconds. It should also be noted that when b is small compared to P_T, the specific rate r_s defined by Eq. (11) becomes $r_s \approx a$. That is, the specific rate is almost independent of P_T.

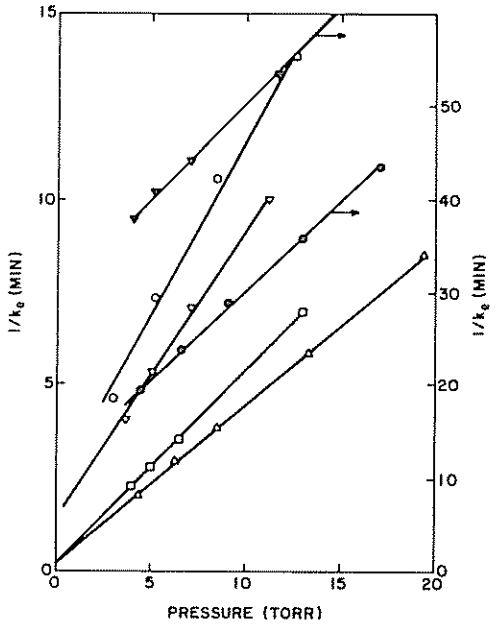

FIG. 8. Dependence of k_{e_o} on the total pressure for the o-H_2/p-H_2 conversion over diamond outgassed at 950°C. Temperature (K): 0, 77; ∇, 90; □, 146; △, 195; ●, 273; ▼, 473.

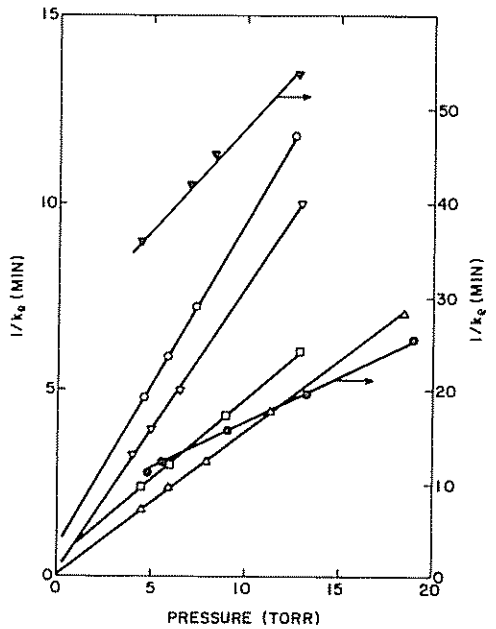

FIG. 9. Dependence of k_e on the total pressure for the HD/H_2/D_2 equilibration over diamond outgassed at 950°C. Temperature (K): O, 77; ∇, 90; □, 146; △, 195; ●, 273; ▼, 385.

TABLE 4

Parameters Giving Dependence of k_s on Pressure for Diamond

Temp (K)	o-H_2/p-H_2			H_2/D_2/HD			Para-magnetic
	a_1[a]	φ_1[a]	b_1[b]	a_2[a]	φ_2[a]	b_2[b]	φ_3[b]
			Outgassed at 950°C				
77	2.28	1.14	3	1.92	1.26	8	0.18
90	2.67	1.52	0.3	2.30	1.57	5.5	0.21
146	4.30	3.05	3	3.84	2.78	1.3	0.33
195	5.26	3.89	1	4.76	3.50	1.6	0.37
273	2.28	1.70	22	1.00	0.76	18	—
385	—	—	—	0.95	0.74	48	—
473	0.95	0.71	41	—	—	—	—
			Covered with Chemisorbed Hydrogen				
77	0.06	0.03					0.03
90	0.08	0.05			Negligible reaction		0.05
146	0.11	0.08					0.08
195	0.13	0.09					0.09
273	0.05	0.04					0.04

[a] In units of 10^{13} molecules/cm^2 · sec.

[b] In units of 10^{16} molecules/cm^2.

It is further concluded that the specific rate of H_2/D_2/HD equilibration is always less than that for the o-p transition under the same conditions. Assuming a negligible isotope effect, the difference can be attributed to the addition of paramagnetic mechanism for the o-p transition. Assuming that all three reactions have the same kinetic form, then

$$(k_s)_3 = (k_s)_1 - (k_s)_2 \tag{52}$$

where $(k_s)_3$ is the paramagnetic contribution, $(k_s)_1$ is the measured rate parameter for the p-o transition, and $(k_s)_2$ is the chemical mechanism rate parameter.

Thus,

$$a_3 \approx a_1 - a_2$$

when b is small or constant for all mechanisms.

The effect of temperature on the specific rate parameters was treated as follows. As discussed in Sec. III, theoretical Eq. (14) suggests that a may contain the term $(1 + 1/K_e)$, K_e being the equilibrium constant of the reaction. Thus, a new specific rate parameter φ was defined by

$$a = \varphi(1 + 1/K_e) \tag{53}$$

or

$$k_s = \frac{\varphi(1 + 1/K_e)}{P_T + b} \tag{54}$$

Table 4 gives values of φ_1, φ_2, and φ_3. The variation of φ as a function of temperature is shown in Figure 10. It should be noted that K_e never differs greatly from 1, so the general conclusions regarding φ as a function of T also apply to a as a function of T. It is concluded that from 77 to 195 K, the temperature effect is small, with a low equivalent activation energy of the order of 0.3 kcal/mole. The values at 273 and 473 K show a pronounced drop, indicating that some new feature is involved in the kinetics. The values of b also show a rapid increase in the same region (see Table 4).

Table 5 gives the kinetic parameters. The results for o-p transition on the diamond sample treated in hydrogen (see Fig. 7) are also shown in Figure 10. The rate of $H_2/D_2/HD$ equilibration on this sample, under comparable conditions, was too small to measure. It is concluded that the o-p conversion in this case is via a paramagnetic mechanism. It would appear that strong chemisorption of hydrogen poisons the chemical mechanism.

Additional results on the effect of chemisorbed gases are shown in Table 6. The surface coverage by gases was estimated by heating to 950°C and measuring the pressure of desorbed gas mass spectrometrically; since this treatment undoubtedly removes only part of the chemisorbed layer, the estimated values are too low (especially for hydrogen). Because the dependence on temperature was

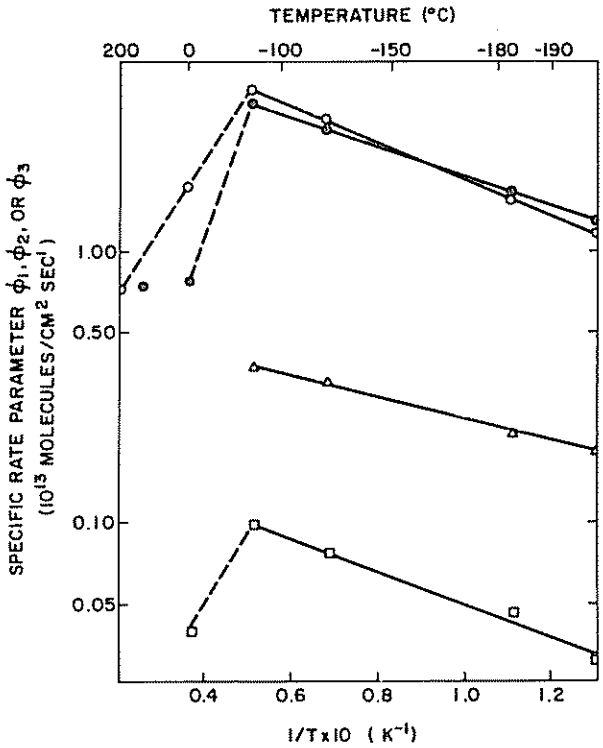

FIG. 10. Arrhenius plots for conversion and equilibration processes over diamond. Sample outgassed at 950°C. Key: O, o-H_2/p-H_2, φ_1; ●, H_2-D_2, φ_2; Δ, paramagnetic, φ_3. Sample covered with chemisorbed hydrogen: □, o-pH_2 (equals paramagnetic). No significant H_2/D_2/HD.

TABLE 5

Kinetic Parameters for Reactions over Diamond Between 77 and 195 K

Sample treatment	Reaction	Equivalent activation energy (kcal/mole)	Preexponential factor (10^{13} molecules/cm^2 · sec)
Outgassed at 950°C	o-H_2/p-H_2	0.3	8.5
	H_2/D_2/HD	0.3	6.8
	Paramagnetic	0.3	1.7
Covered with chemisorbed hydrogen	o-H_2/p-H_2 (paramagnetic)	0.3	0.02
	H_2/D_2/HD	Rate too low to measure	Rate too low to measure

TABLE 6

Comparison of specific rates at 77 K with ESR Measurements on Diamond Surfaces

Surface treatment	Estimated surface coverage (10^{15} atoms/cm^2)	Unpaired spins[a] (10^{13} cm^{-2})	Specific rate, r_s (10^{11} molecules/cm^2 · sec)	
			p-H_2	HD/H_2/D_2
With hydrogen (900°C)	0.7	1.1	0.4	<0.01
With chlorine (400°C)	0.6	4.1	0.8	<0.01
With oxygen (400°C)	1.2	2.1	135	<0.01
Outgassed at 950°C	1	3.5	205	157

[a]Data from Sappok and Boehm [48].

not measured for all of these samples, the results are given as comparative specific rates r_s, at P_T = 7 torr, T = 77 K. However, plots of $1/k_e$ versus P_T (see Fig. 8) showed that the intercept was usually near zero for all of these results at 77 K. The specific rate r_s is almost independent of pressure and can be equated to a in Figures 11 and 12.

It is concluded that chemisorbed species cover nearly all the surface; that this eliminates any chemical mechanism since H_2/D_2/HD equilibration is very slow; and that the paramagnetic o-p conversion rate is also reduced for the case of chemisorbed hydrogen or chlorine, but for oxygen the paramagnetic conversion rate is almost as high as for the chemical mechanism on the outgassed sample.

Mixtures of paramagnetic and chemical mechanisms were studied by partially degassing the treated samples and measuring o-p transition and H_2/D_2/HD equilibration at 77 K, P_T = 7 torr, on the partially degassed samples. The rate of paramagnetic conversion was estimated by subtracting the H_2/D_2/HD rate from the o-p rate. The results are shown in Figures 11-13. For chlorine-treated samples, removal of adsorbed chlorine increased the o-p rate in close relation to the amount removed. Figure 14 shows the relation; the intercept of the upper straight line corresponds to the paramagnetic rate, under these conditions, for the outgassed sample (see Table 6). It might be tentatively concluded that as chlorine is desorbed, both the paramagnetic and chemical rates increase

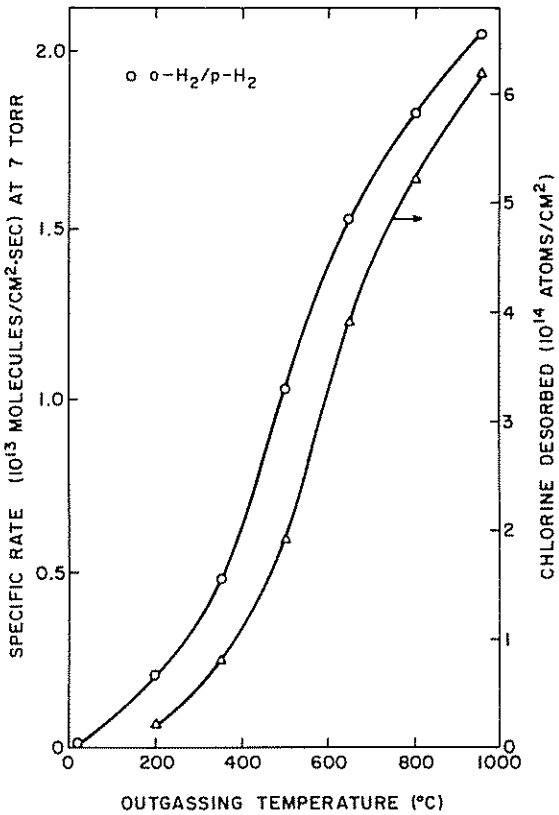

FIG. 11. Effect of outgassing temperature on the conversion rate at 77 K over diamond previously treated with chlorine.

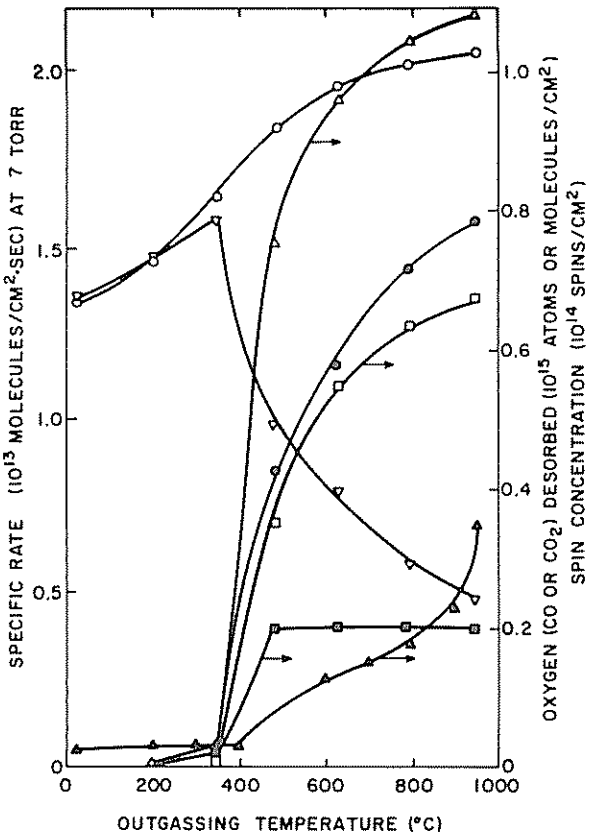

FIG. 12. Effect of outgassing temperature on the conversion and equilibration rates at 77 K and ESR over diamond previously treated with oxygen. Key: ○, conversion; ●, equilibration; ▽, paramagnetic conversion; △, total oxygen desorbed; □, CO desorbed; ▪, CO_2 desorbed; ▲, spin intensity.

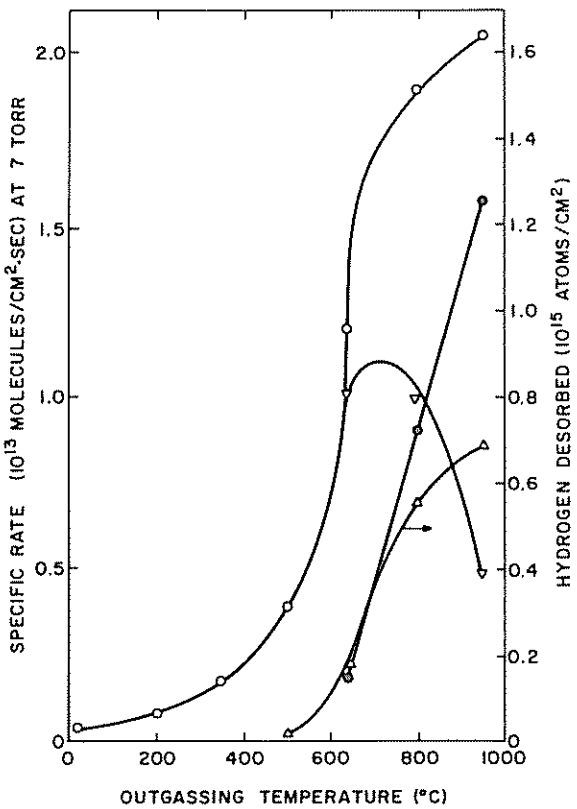

FIG. 13. Effect of outgassing temperature on the conversion and equilibration rates at 77 K over diamond previously treated with hydrogen. Key: O, conversion; ●, equilibration; ▽, paramagnetic conversion; △, hydrogen desorbed.

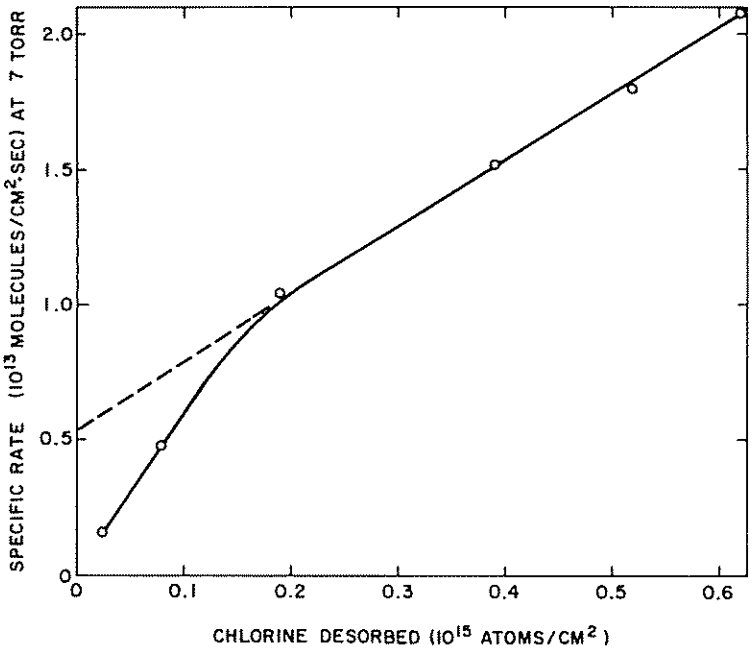

FIG. 14. Change in specific rate of conversion at 77 K over diamond with amount of chlorine desorbed by heat treatment.

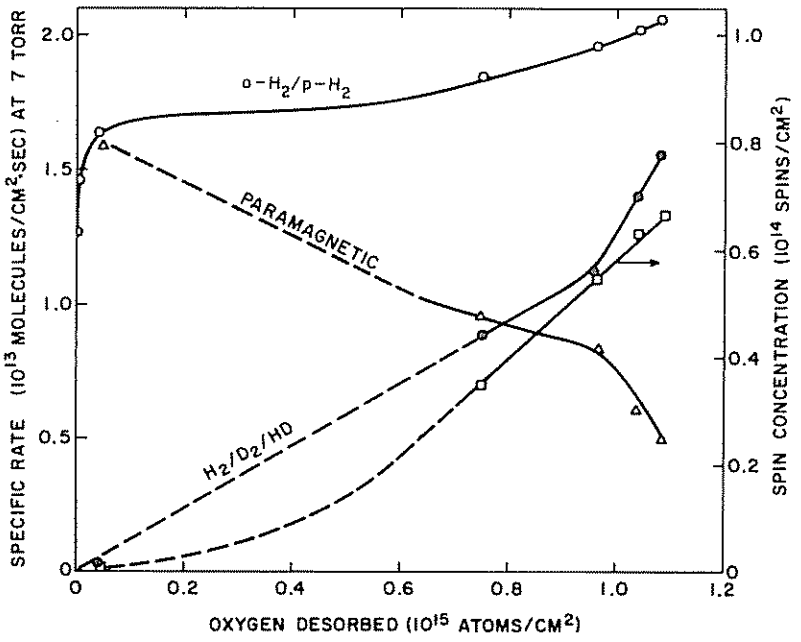

FIG. 15. Change in specific rates of conversion and equilibration at 77 K and ESR over diamond with amount of oxygen desorbed (as CO plus CO_2) by heat treatment.

linearly, but the paramagnetic rate reaches a maximum when 0.2×10^{15} chlorine atoms/cm^2 have been removed. Figure 15 shows the result for desorption of oxygen. Again, it would appear that the chemical conversion rate increases roughly linearly as oxygen is desorbed, but the paramagnetic conversion rate also decreases roughly linearly, so that the total o-p rate varies only by a factor of 1.5 over the complete range of surface coverage. It can be seen from Figures 12 and 15 that the spin concentration also increases as oxygen is desorbed. It might be concluded that desorption of oxygen freed unpaired electrons to the extent of about 1/20 electron per oxygen atom.

Figure 16 summarizes the results for the relation between rates over diamond and amount of hydrogen desorbed. The equilibration (or chemical conversion) rate increases sharply with increasing amounts of hydrogen removal. However, unlike the case of the surface contaminated with oxygen, the conversion reaction also increases sharply with complex removal. Thus, the contribution from the paramagnetic conversion decreases more slowly with hydrogen complex removal than is the case with oxygen complex removal.

Figure 17 shows hydrogen isotherms on the sample degassed at 950°C. No detectable adsorption was found at 273 K. Using the Clapeyron-Clausius equation, the isosteric heat of adsorption is estimated to be 0.5 kcal/mole for coverages between 0.01×10^{15} and 0.03×10^{15} molecules/cm^2. It is concluded that the rate measurements on degassed diamond described above are for fractional coverages less than 0.1, based on the BET area.

B. Over Graphon

As for diamond, the results fit the first-order expression of Eq. (43) for all conditions studied, including temperatures up to 800 K. As before, the possibility of a diffusion effect was investigated, but no change in specific rate r_s was observed as the sample weight was changed from 420 to 60 mg.

The pressure dependence of Eq. (51) was again observed (see Figs. 18 through 20) as a reasonable first approximation. Figure 20 is for Graphon reacted in oxygen to about 16% burn-off and then degassed at various temperatures. The

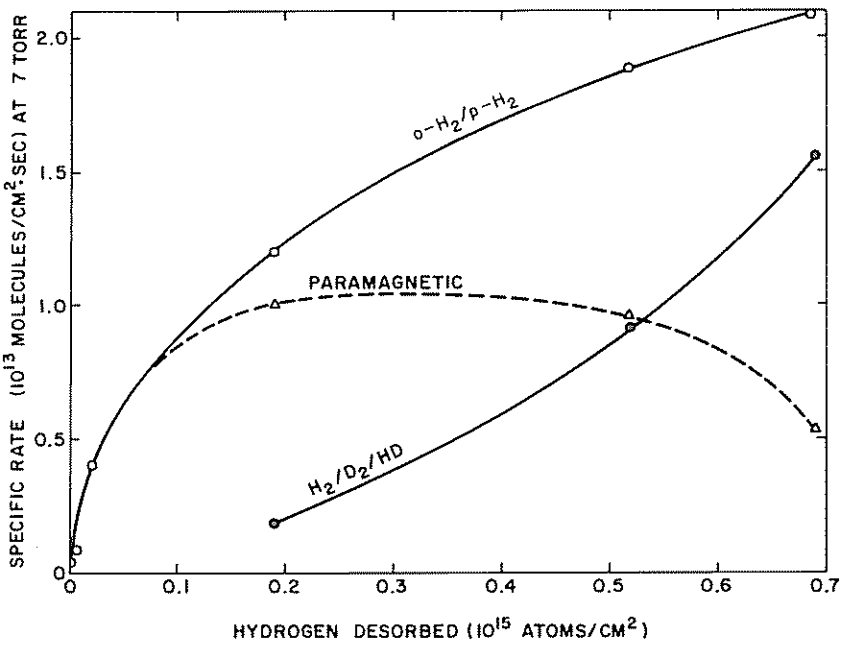

FIG. 16. Change in specific rates of conversion and equilibration at 77 K over diamond with amount of hydrogen desorbed by heat treatment.

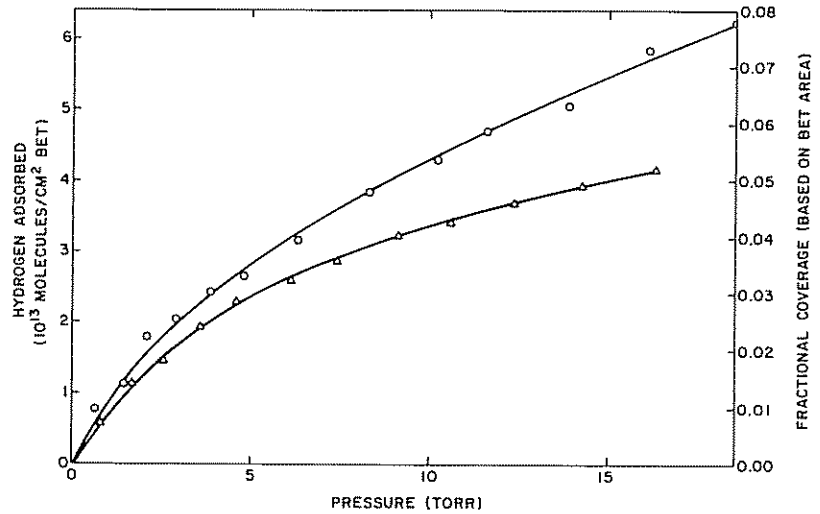

FIG. 17. Isotherms for hydrogen adsorption on diamond outgassed at 950°C. Adsorption temperature (K): O, 77; Δ, 90.

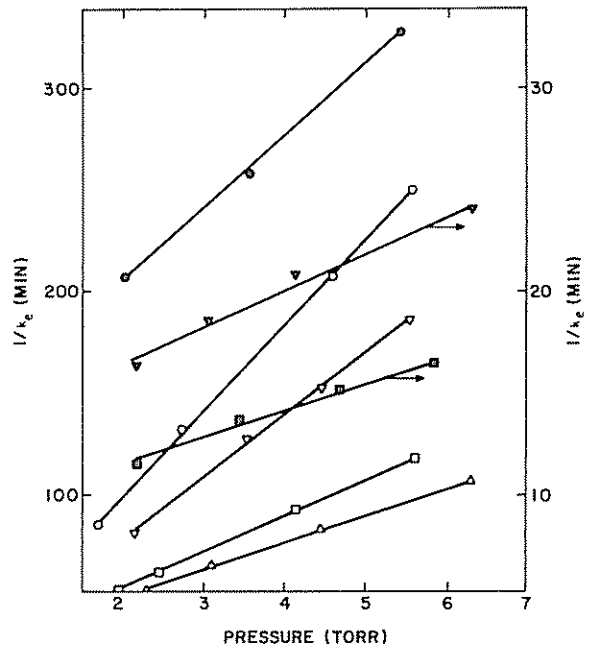

FIG. 18. Dependence of k_e on the total pressure for the o-H_2/p-H_2 conversion over original Graphon outgassed at 950°C. Temperature (K): O, 77; ▽, 90; □, 146; △, 195; ●, 297, ▼, 633; ■, 773.

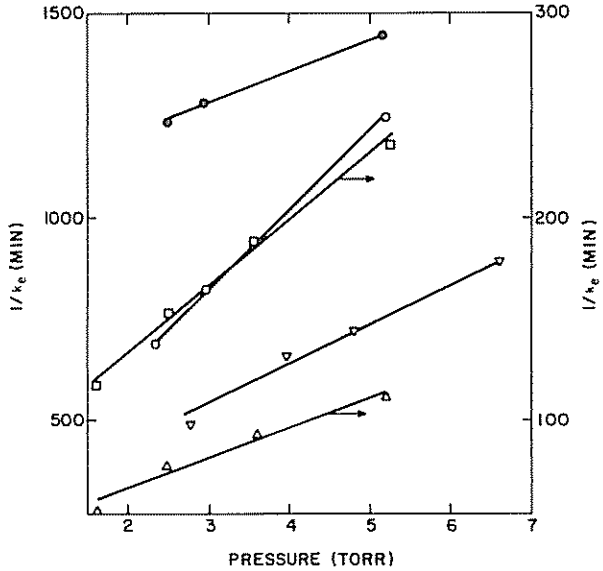

FIG. 19. Dependence of k_e on the total pressure for the H_2/D_2/HD equilibration over original Graphon outgassed at 950°C. Temperature (K): O, 77; ▽, 90; □, 146; △, 195; ●, 297.

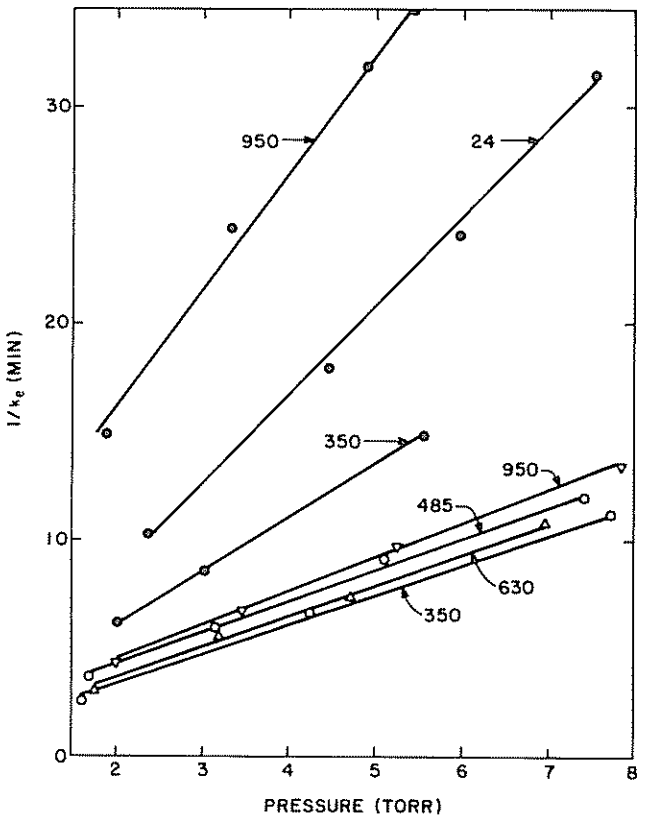

FIG. 20. Dependence of k_e on the total pressure at 77 K over 16% burn-off Graphon samples containing various amounts of oxygen (outgassing temperature indicated in °C): O △ ▽, o-pH_2; ●, $H_2/D_2/HD$.

sample at 16% burn-off was also annealed at 1700°C in nitrogen for 15 min and outgassed at 950°C. The same first-order rate expression and form of pressure dependence were obtained with this sample. The specific rate parameters a, b, and φ are given in Table 7.

The temperature dependence of φ values is shown in Figure 21 for the original Graphon sample and for outgassed Graphon at 16% burn-off, annealed and nonannealed. The results are similar in form to those described above for diamond, but because higher temperatures were also investigated the results show the presence of a new region in the Arrhenius plot. Because of experimental

TABLE 7

Kinetic Parameters for Graphon Outgassed at 950°C

Temp (K)	o-H_2/p-H_2			H_2/D_2/HD			Para-magnetic
	a_1[a]	φ_1[a]	b_1[b]	a_2[a]	φ_2[a]	b_2[b]	φ_3[a]
			Original Graphon				
77	0.20	0.10	1.1	0.10	0.03	4.1	0.07
90	0.26	0.15	1.8	0.0075	0.05	9.2	0.10
146	0.45	0.32	3.7	0.26	0.19	8.2	0.14
195	0.63	0.46	6.0	0.51	0.37	10.2	0.09
297	0.14	0.11	13.0	0.11	0.08	57	—
453	0.03	0.02	—	—	—	—	—
483	—	—	—	0.02	0.017	—	—
633	38	29	23	—	—	—	—
773	63	47	23	8.2	6.6	—	—
			16% Burn-off nonannealed				
77	4.1	2.0	7.5	1.2	0.8	14	1.4
90	4.5	2.6	13	1.9	1.3	9	1.5
146	8.4	6.0	15	6.1	4.4	12	1.6
195	11.0	8.1	—	9.6	7.0	17	1.1
273	5.3	4.0	20	1.4	1.1	—	—
600	—	—	0.6	0.6	0.5	—	—
673	3.8	3.0	33	—	—	—	—
773	—	—	—	6.2	4.9	22	—
823	14.6	10.9	33	—	—	—	—
			16% Burn-off annealed at 1700°C				
77	2.0	1.0	1.0	0.6	0.4	22	0.7
90	2.5	1.4	—	1.0	0.7	14	0.8
146	5.2	3.7	11	3.6	2.6	26	1.1
195	6.7	5.1	12	6.6	4.8	20	0.2
228	6.0	4.5	17	—	—	—	—
297	4.4	3.3	14	2.1	1.6	—	—
418	2.2	1.7	7	—	—	—	—
543	3.4	2.6	52	0.7	0.5	—	—
610	—	—	—	1.2	0.9	—	—
673	3.8	2.9	30	—	—	—	—
797	7.8	5.9	34	8.0	6.3	—	—

[a] In units of 10^{12} molecules/cm^2 · sec.

[b] In units of 10^{15} molecules/cm^3.

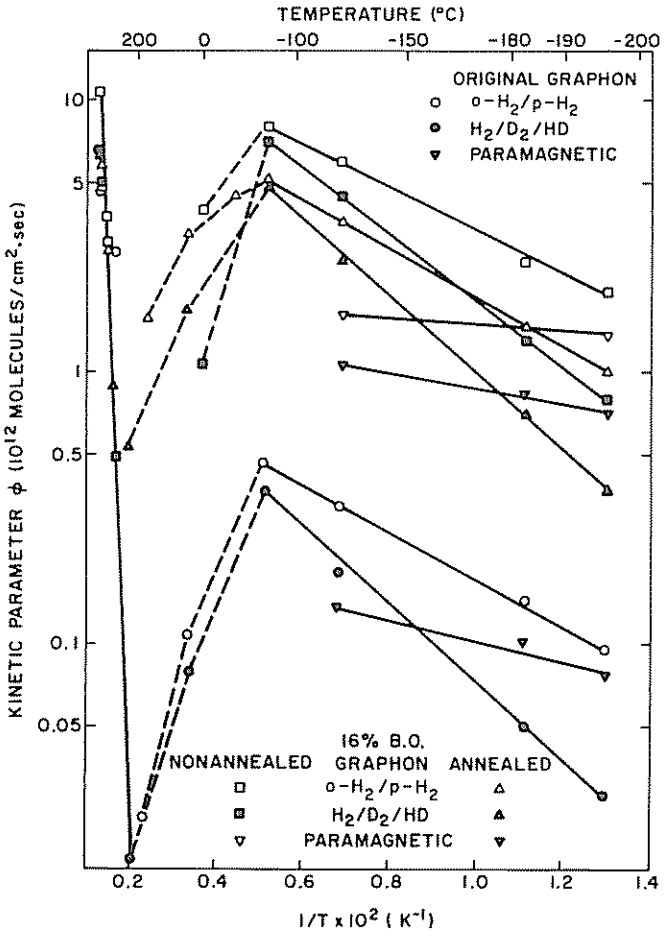

FIG. 21. Arrhenius plots for conversion and equilibration processes over Graphon (B.O. denotes burn-off).

variability and insufficient data, it is not possible to distinguish o-p transition rates from $H_2/D_2/HD$ rates in this higher-temperature region. Thus, a single set of specific rate parameters is assigned (see Table 8).

Treatment of Graphon with oxygen at 350°C produced a radically different effect on rates at 77 K than that observed with diamond (compare Fig. 22 with Fig. 12). The $H_2/D_2/HD$ equilibration could not be measured on the oxygen-treated Graphon until the degassing temperature exceeded 600°C, even though significant desorption of CO and CO_2 started at 400°C. (Note that the oxygen per centimeter^2 BET area desorbed at 950°C is two orders of magnitude lower for the Graphon than for diamond.) In addition, only a small o-p rate was found for the Graphon sample covered with maximum oxygen.

Similar results were obtained for Graphon samples taken to various degrees of burn-off before oxygen treatment (see Figs. 23 and 24). However, even a small degree of burn-off (3.7%) is capable of producing a surface which has a

TABLE 8

Kinetic Parameters for Reactions over Graphon Samples Outgassed at 950°C

Temp (K)	Graphon (% B.O.)[a]	Reaction	Equivalent activation energy (kcal/mole)	Preexponential factor (10^{12} molecules/ cm^2 · sec)
77 to 200	0.0	o-H_2/p-H_2	0.4	1.2
		$H_2/D_2/HD$	0.6	1.8
		Paramagnetic	0.2	0.04
	15.9	o-H_2/p-H_2	0.4	20
		$H_2/D_2/HD$	0.5	30
		Paramagnetic	0.06	2.0
	15.9	o-H_2/p-H_2	0.3	8
	(Annealed)	$H_2/D_2/HD$	0.6	22
		Paramagnetic	0.1	2.5
>450	All samples	o-H_2/p-H_2	13.6	4.2×10^4
		$H_2/D_2/HD$		

[a] B.O. denotes burn-off.

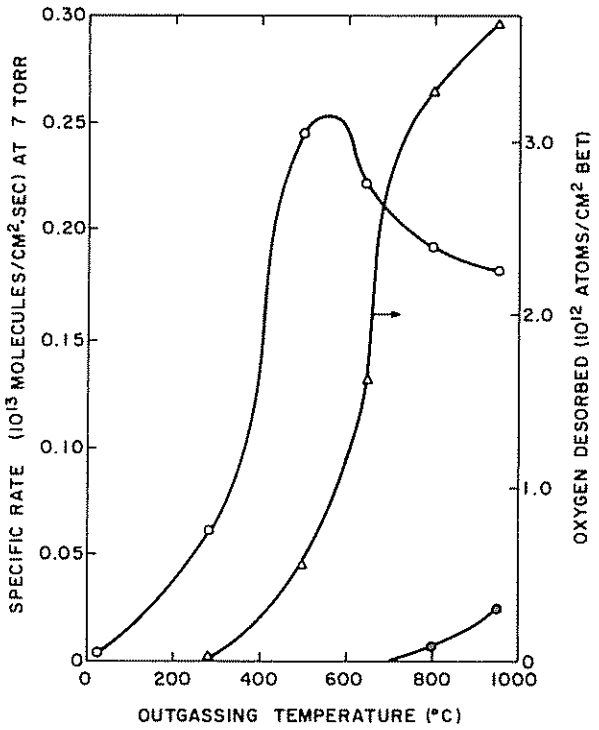

FIG. 22. Effect of outgassing temperature on the conversion and equilibration rates at 77 K over original Graphon previously treated with oxygen: O, conversion; ●, equilibration; △, oxygen desorbed (as CO plus CO_2).

significant initial o-p rate despite no desorption of oxygen-containing gases. Figure 25 shows the relation between chemisorbed oxygen and burn-off. Figures 23 and 24 indicate that although the quantities of chemisorbed oxygen vary with sample burn-off, as shown by Figure 25, the form of the variation of o-p and $H_2/D_2/HD$ rates with coverage is similar for all cases, but rates are lower for lower burn-offs. Since the active site area per centimeter^2 BET area varies in the same order as the rates, the results were replotted as rate per ASA vs oxygen desorbed per ASA (see Fig. 26). It is concluded that except for the o-p reaction on the original Graphon with no burn-off, all the specific rates on this basis were the same function of oxygen desorbed per ASA.

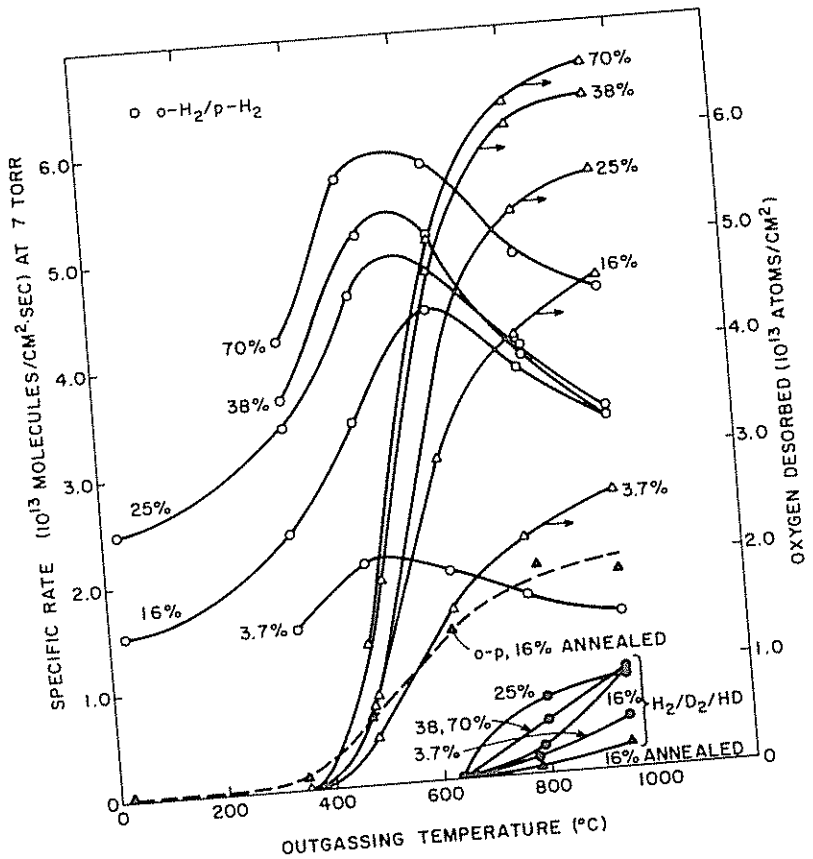

FIG. 23. Effect of outgassing temperature on the conversion and equilibration rates at 77 K over Graphon samples of different burn-offs. Samples previously treated with oxygen.

Figure 24 also shows data for a 16% burn-off Graphon, heat annealed for 15 min at 1700°C before oxygen treatment, at various stages of oxygen removal. Annealing obviously reduces the number of active sites and, hence, oxygen adsorption. The rates decrease accordingly. However, annealing also produced the low initial value of o-p conversion noted with the original Graphon.

Table 9 summarizes the kinetic parameters at 77 K for Graphon samples of various burn-offs, exposed to oxygen, and then degassed at various temperatures.

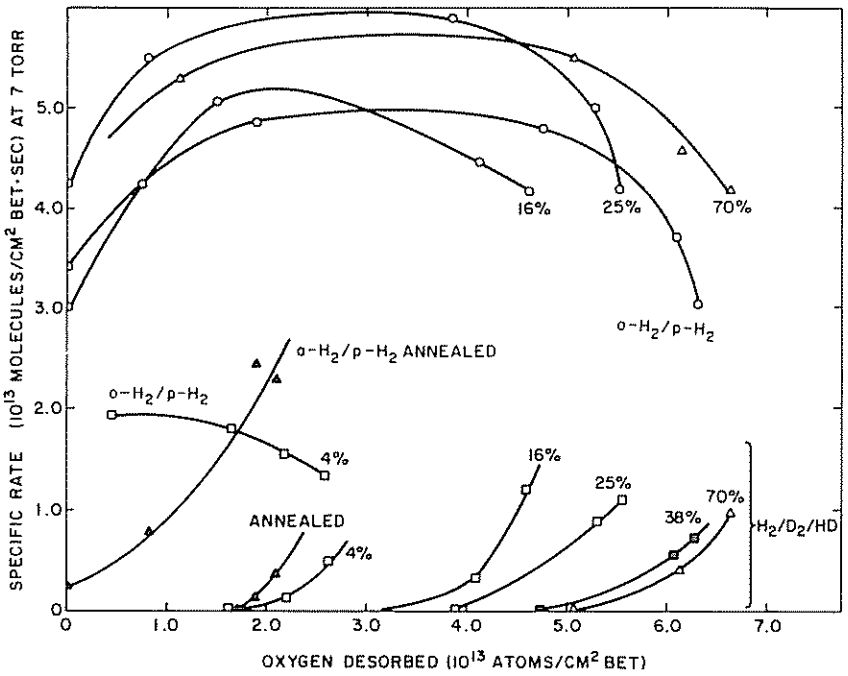

FIG. 24. Change in specific rates of conversion and equilibration at 77 K over Graphon samples of different burn-off with amount of oxygen desorbed (as CO and CO_2).

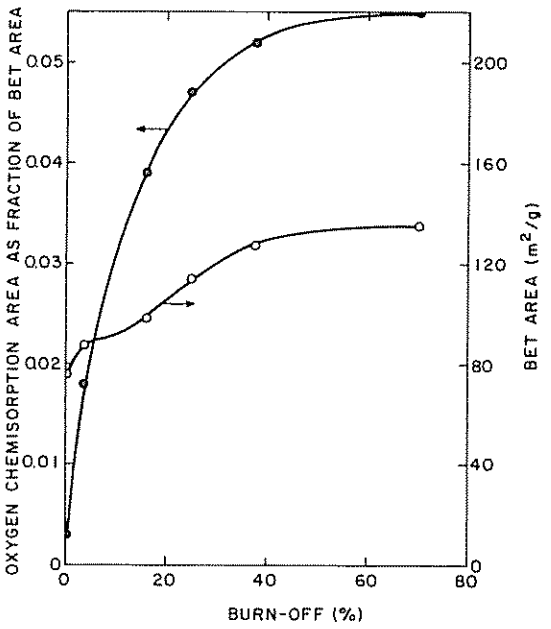

FIG. 25. Change in total (BET) area and active (ASA) area of Graphon with burn-off.

TABLE 9

Kinetic Parameters at 77 K for Graphon Samples of Various Burn-Offs, Exposed to Oxygen, and Degassed at Various Temperatures

Case	Outgassing temperature	o-H_2/p-H_2 conversion[a]		H_2/D_2/HD equilibration[a]		Paramagnetic[a]
		a_1	φ_1	a_2	φ_2	φ_3
Original Graphon	25	0.07	0.04	—	—	0.04
	270	0.14	0.07	—	—	0.07
	500	0.25	0.12	—	—	0.12
	640	0.24	0.12	—	—	0.12
	800	0.21	0.10	0.03	0.02	0.09
	950	0.20	0.10	0.04	0.03	0.08
3.7% B.O.	350	1.6	0.8	—	—	0.8
	490	2.3	1.2	—	—	1.2
	640	2.2	1.1	—	—	1.1
	790	2.0	1.0	0.16	0.10	0.9
	960	1.6	0.8	0.35	0.23	0.7
16% B.O.	25	1.5	0.8	—	—	0.8
	350	2.6	1.3	—	—	1.3
	490	4.4	2.2	—	—	2.2
	630	4.7	2.4	0.03	0.02	2.3
	790	4.5	2.2	0.3	0.2	2.1
	950	4.1	2.1	1.2	0.8	1.5
25% B.O.	25	2.7	1.3	—	—	1.3
	350	3.8	1.9	—	—	1.9
	480	5.1	2.6	—	—	2.6
	630	5.3	2.7	0.01	0.007	2.7
	790	4.5	2.2	1.0	0.7[b]	1.7
	950	3.8	1.9	1.3	0.9[b]	1.2
38% B.O.	350	3.9	2.0	—	—	2.0
	510	5.5	2.7	—	—	2.7
	640	4.9	2.5	—	—	2.5
	790	4.3	2.2	0.4	0.3[b]	2.0
	960	3.8	1.9	1.1	0.8[b]	1.4
70% B.O.	350	4.9	2.4	—	—	2.4
	470	6.3	3.2	—	—	3.2
	640	6.7	3.3	—	—	3.3
	800	6.0	3.0	0.5	0.3[b]	2.8
	950	5.0	2.5	1.1	0.7	2.0

[a] Parameters in units of 10^{12} molecules/cm^2 · sec.

[b] High.

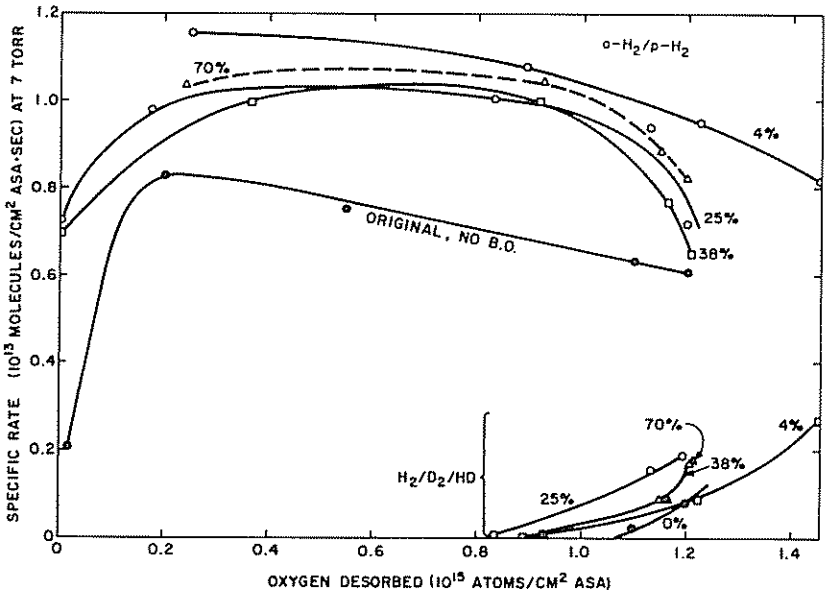

FIG. 26. Change in specific rates of conversion and equilibration at 77 K over Graphon samples of different burn-offs with amount of oxygen desorbed (as CO plus CO_2). Both rates and oxygen desorbed expressed per unit of ASA (B.O., burn-off).

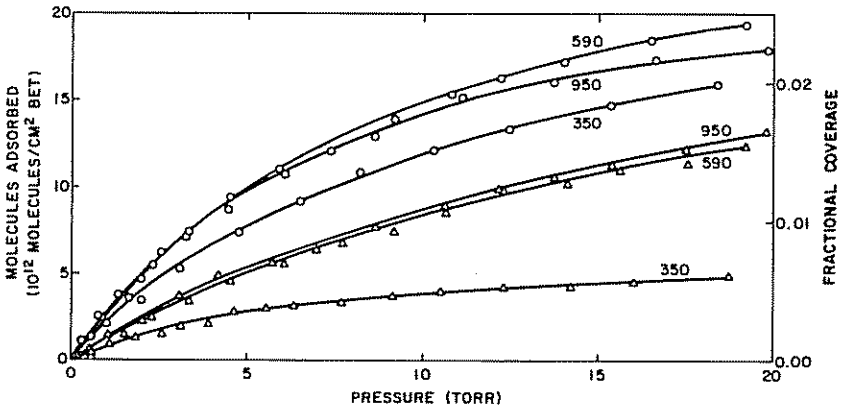

FIG. 27. Isotherms for hydrogen adsorption on 16% burn-off Graphon following oxygen removal at 350, 590, and 950°C. Adsorption temperature (K): O, 77; Δ, 90.

Figure 27 shows hydrogen adsorption isotherms for the 16% burn-off Graphon with and without chemisorbed oxygen. No adsorption was detected at 273 K. Although Figure 22 indicates that there is still a significant fraction of adsorbed oxygen left after degassing at 590°C, the isotherms for this sample are virtually identical to that for the sample degassed at 950°C. The sample degassed at 350°C has lost little chemisorbed oxygen, but the quantity of hydrogen adsorbed (at 77 K) is almost as great as for the degassed sample.

VI. DISCUSSION OF RESULTS AND CONCLUSIONS

A. Diamond

It is of interest to consider the basic surface structure of diamond in terms of free valencies before interpreting the experimental results. In an ideal, undistorted (111) crystal face of diamond there would be a free bond per 5.51 $\AA^2$; in the (110) face, there would be one per 4.50 $\AA^2$; and in the (100) face, there would be one per 3.18 $\AA^2$. The arrangement of atoms in the (111), (110), and (100) faces is shown in Figure 28.

The calculation of frequency for each plane was made assuming that the specific surface energy is proportional to the number of free valencies per unit area and that there is an exponential relationship of exposed surface area and specific surface energy [75]. As shown in Table 10, for 1 cm^2 of diamond, 2.0×10^{15} free valencies at 1.9×10^{15} carbon atoms would be expected. On the (100) surface, the interaction between two free valencies is likely to produce rehybridization, and the most probable valencies are based on the divalent configuration s^2p^2 of a lone electron pair [33].

These figures seem to agree quite well with the interpretation of chemisorption of oxygen on diamond, as put forth by Sappok and Boehm [48, 49]. They observed that 1.17×10^{15} oxygen atoms could be chemisorbed on 1 cm^2 of diamond surface and that infrared spectra indicate the presence of carbonyl groups and ether-like bound oxygen. It was concluded that oxygen chemisorbs on the (111) and (110) surfaces with an ether structure (-C-O-C-) and on the (100) surface with a carbonyl structure (C=O).

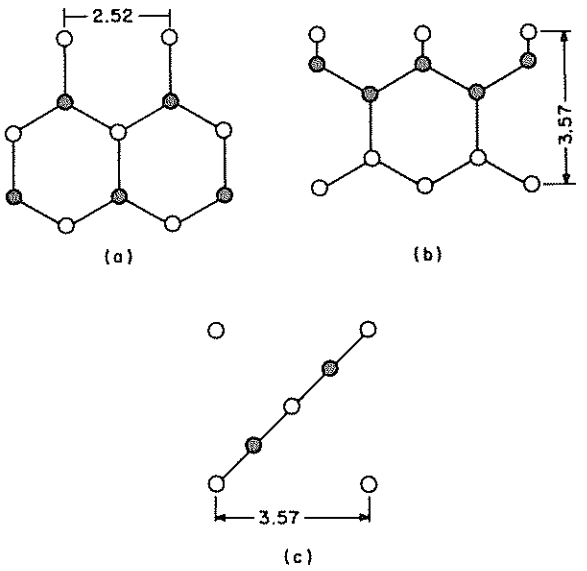

FIG. 28. Arrangement of atoms in diamond (a) (111), (b) (110), (c) (100) surfaces. Figures indicate carbon-carbon spacings in angstroms. Open circle, carbon atoms in the surface. Closed circle, carbon atoms beneath the surface.

TABLE 10

Physical Properties of Three Diamond Crystal Faces

No. of bonds cut/atom	Area ($Å^2$)	Frequency (%)	Expected surface atoms/cm^2 of diamond powder	Expected free valencies/cm^2 $\times 10^{-15}$
100/2	6.36	10.4	0.15	0.30
110/1	4.50	33.5	0.75	0.75
111/1	5.51	56.1	1.0	1.0

If their conclusion on the presence of these surface groups is applied to our calculation of expected surface free valencies, that is, one oxygen atom saturates two surface free valencies, 1.03×10^{15} oxygen atoms are expected to chemisorb on 1 cm^2 of diamond surface. The small discrepancy between this figure and that found experimentally by Sappok and Boehm may arise from the presence of another surface group in which an oxygen atom does not saturate two free valencies, but one. The presence of ionized oxygen atoms on the (111) surface ($-C-O^-$) is likely and will be discussed later.

All the kinetic results very well fit the expression

$$X(t) - X(\infty) = [X(0) - X(\infty)] \exp(-k_e t) \tag{43}$$

where $X(\infty)$ is the calculated equilibrium molar fraction. This means that the rate of reaction per unit BET area is given by

$$r(t) = \frac{k_e P_T V}{A} [X(t) - X(\infty)] \qquad \text{molecules/cm}^2 \cdot \text{sec} \tag{47}$$

A "specific rate" can be defined by setting $X(t) - X(\infty)$ equal to 1,

$$r_s = \frac{k_e P_T V}{A} \qquad \text{molecules/cm}^2 \cdot \text{sec} \tag{55}$$

and a specific rate constant can be defined, as shown in Eq. (12), by

$$k_s = \frac{k_e V}{A} \qquad \text{cm/sec}$$

It was found that, as a reasonable approximation, the variation of k_s with total pressure (since the total pressure affects the degree of surface coverage with adsorbed ortho- and parahydrogen or H_2, D_2, HD) was of the form [Eq. (50)

$$k_s = \frac{a}{P_T + b}$$

A theoretical treatment, assuming simple Langmuir adsorption kinetics to apply, gives a rate expression of the correct form [Eq. (43)], with

$$k_s = \frac{1}{1 + K_1 P_T} \frac{C_s k_a k_f (1 + 1/K_e)}{k_d + k_f + k_b} \tag{56}$$

$$k_s = (1 - \theta) \frac{C_s k_a k_f (1 + 1/K_e)}{k_d + k_f + k_b} \tag{57}$$

for a paramagnetic mechanism involving nondissociative adsorption. All the chemical mechanisms investigated led to the correct form of Eq. (43). However, the Eley-Rideal mechanism can be ruled out because it produces θ in place of the $1 - \theta$ term of Eq. (57); hence, k_s would increase with P_T or would be constant if $\theta \to 1$, whereas all the results showed k_s to decrease with higher P_T. Any mechanism which produces $k_s \propto f(1 - \theta)$ is feasible, but the experimental results,

which fit Eq. (50), are consistent with $f(1 - \theta) \approx 1 - \theta$ rather than the more complex functions expected.

Because of the forms of Eqs. (50) and (57), k_s was expressed as

$$k_s = \frac{\varphi(1 + 1/K_e)}{P_T + b} \tag{54}$$

and the temperature dependencies of φ and b were investigated. As b increases, θ decreases [$\theta = P_T/(P_T + b)$, Eq. (22)]; φ should be relatively independent of the variation in θ with temperature.

The results for diamond (Table 4) showed that the o-p conversion and the $H_2/D_2/HD$ equilibration had closely similar specific rates, demonstrating a chemical mechanism as predominant in the o-p conversion. The equivalent activation energies for chemical conversion, equilibration, and paramagnetic conversion are all low, less than 0.3 kcal/mole, demonstrating that the slow step in the chemical reactions does not involve a high activation energy of splitting the hydrogen molecule. Although the values of b cannot be accurately determined and show considerable variability, they indicate that at the pressures used θ was close to 1 at low temperatures but decreased sharply at 273 K. Figures 8 and 9 show that the rate constant k_s decreased at these temperatures. Part of this decrease was due to the decrease of θ as shown by the higher b values, but Figure 10 also indicates a decrease in the specific rate constant φ.

The most likely reason for this is that there are two types of sites involved, so that

$$k_s = \frac{\varphi_1(1 + 1/K)}{P_T + b_1} + \frac{\varphi_2(1 + 1/K)}{P_T + b_2} \tag{58}$$

Due to a larger activation energy or a smaller value of C_s, type 2 sites would have a small value of θ_2 at low temperatures, so that the results are dominated by type 1 sites. However, as temperature is raised a point is reached where the value of θ_1 is no longer near 1, and the next higher temperature tested gives a high value of b_1 and low θ_1. Without type 2 sites this would lead to a small value of k_s, but type 2 sites come into play and dominate the value of k_s. The values of b at the higher temperatures indicate a low value of θ_2. This line of reasoning

would predict that both φ and b should increase with further increase of temperature, probably with a higher activation energy for φ_2. Alternatively, desorption of strongly adsorbed, gas-blocking type 2 sites might also account for them coming into play at higher temperatures.

It is not possible to compare the values of the preexponential factor for φ_1 with theoretical expressions because it contains the unknown factor C_s, the number concentration of active sites. However, since the chemical mechanisms operate via adsorbed gas at $\theta \to 1$ (at $P_T = 7$ torr, low temperatures), the concentration of active sites must certainly be less than the corresponding total surface coverage by hydrogen at these conditions. Figure 17 indicates a coverage of about 0.04 fraction at these conditions or C_s less than the order of $(0.04)(2)(10^{15}) \approx 10^{14}$ sites/cm^2. The measured preexponential factor of about $(8)(10^{14})$ molecules/cm^2 · sec indicates, as usual in results on conversion-equilibration, either that the number of active sites is very much lower than the quantity of adsorbed hydrogen, or that there is a large entropy of activation in the transition.

The adsorption of hydrogen at high temperatures followed by cooling and testing at 77 K virtually eliminates the chemical mechanism. The estimated surface covered by chemisorbed H, approximately 10^{15} atoms/cm^2, is probably close to saturation. The paramagnetic results are also reduced (see Tables 4 and 6) both by lower φ and by higher b (lower θ values). This is strong evidence that dissociative adsorption of hydrogen either blocks the sites active for the chemical mechanism or prevents mobility of weakly adsorbed species over the surface. Therefore, any chemical mechanism involving chemisorbed dissociated atoms appears to be unlikely, unless it is postulated (a) that an active site can dissociatively chemisorb weakly at low temperatures but strongly (firmly bonded) at high temperatures, thus being poisoned, or (b) that dissociatively chemisorbing weak sites still exist after high-temperature hydrogen adsorption but can no longer promote reaction because they cannot be reached by mobile weakly adsorbed species. In case b, it is presumably not chemisorbed H atoms which are mobile since it would be expected that these would proceed to adsorb firmly on strong-bonding sites, in the first results without high-temperature H_2 treatment, thus also poisoning the surface.

Adsorption of chlorine or oxygen also poisons the chemical mechanism. Chlorine appears to behave similarly to hydrogen, but oxygen greatly increases the paramagnetic conversion rate, almost to the level of the chemical mechanism on the untreated surface. No relation to unpaired-spin concentration is apparent. The chemical mechanism was partially restored as the samples were outgassed. It appears that with H_2- and Cl_2-treated samples a fractional removal of coverage completely restores the paramagnetic conversion, and even enhances it, whereas the chemical mechanism increases steadily as more poisoning gas is removed. This indicates that (a) the paramagnetic sites are poisoned by the more weakly adsorbed fractions of the poisoning gas, and (b) the adsorption involved in the chemical mechanism may itself poison paramagnetic conversion.

For O_2-treated diamond, an increase in the rate of paramagnetic conversion is accompanied by desorption of water and CO_2, and the rate reaches a maximum at an outgassing temperature of 350°C. Further removal of oxygen atoms causes a decrease in the rate of paramagnetic conversion, while the rate of equilibration increases and is roughly proportional to the number of CO molecules absorbed. This suggests that the same paramagnetic mechanism is operating on the diamond with different amounts of surface oxygen complex. Therefore, the change in the rate of paramagnetic conversion must come from the change in the number of paramagnetic sites.

The number of unpaired electrons determined by ESR starts to increase at an outgassing temperature of 400°C; the desorption of CO also increases, as seen in Figure 12. In contrast, the rate of paramagnetic conversion starts to decrease. Thus, the desorption of CO molecules seems to involve the removal of paramagnetic centers active in conversion, while at the same time active sites for the equilibration are created, together with unpaired electrons sensitive for ESR. This leads to the conclusion that there are two kinds of paramagnetic sites present on a diamond partially covered with chemisorbed oxygen; one is responsible for the paramagnetic conversion and the other is responsible for the ESR signal.

The paramagnetic site for the conversion may be identified with chemisorbed oxygen itself. Some fraction of chemisorbed oxygen on the (111) surface may ionize to form paramagnetic $-C-O^-$, which would be effective in bringing about the o-p transition. This paramagnetism would not be observed by ESR if the

lifetime of this species were less than the order of 10^{-9} sec [76]. Based on the estimate of de Boer [77], when the heat of adsorption is about 0.5 kcal/mole, the average lifetime of the hydrogen molecule on the diamond surface would be 1.4×10^{-11} sec. This sets a lower limit on the time during which the conversion can occur on the surface. Therefore, if the lifetime of this species were between 10^{-9} and 10^{-11} sec, this species would not be observed by ESR, but would be effective for the conversion. The assumption of the existence of this kind of species on a diamond structure is not unreasonable, since on germanium the initial increase in conductivity by chemisorption of oxygen can be explained by the existence of this species (the oxygen chemisorbed as O^-)[78]. The magnetic moment of this species has not yet been determined, but based on the observation that the magnetic moment of O_2^- in potassium superoxide is close to that of the free electron [79], it is reasonable to assume that the magnetic moment of $-C-O^-$ is also close to that of the free electron.

It is known that addition of water causes a decrease in the conversion rate at low temperatures [80, 81]. The sites active at low temperatures are considered to be particularly susceptible to water. Sappok and Boehm [48] found that the number of hydrophilic centers for water adsorption on diamond increases from 0.57×10^{14} cm^{-2} for a sample outgassed at 900°C to $1.9 \times 10^{14}/cm^{-2}$ for a sample with chemisorbed oxygen. This hydrophilic center may be identified with an ionized oxygen chemisorbed on diamond.

The inability to catalyze the equilibration on the (111) surface with the paramagnetic oxygen ion is probably due to the absence of interaction between paramagnetic sites because of the low probability of finding two adjacent paramagnetic oxygen ions. Turkevich and Laroche [31] have suggested that the catalytic activity for the equilibration is not associated with the presence of isolated noninteracting electrons but rather with a pool of interacting electrons. Sappok and Boehm [49] concluded that the ether group (-C-O-C-) is expected mainly on the (111) surface with chemisorbed oxygen. According to the previous calculation, there are 1.0×10^{15} surface carbon atoms per cm^2 in the (111) surface, while the total number of paramagnetic sites is only 1.9×10^{14} cm^{-2}. This is only 20% of the number of surface carbon atoms in the (111) surface. It is likely that all these paramagnetic sites are randomly distributed on the (111) surface. Three possible modes of oxygen adsorption are shown in Figure 29.

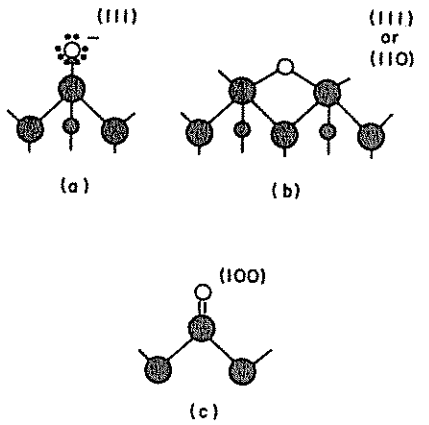

FIG. 29. Possible modes of O_2 adsorption. (a) Oxygen chemisorbed as O^-, (b) oxygen chemisorbed ether-like with the removal of two free valencies, (c) oxygen chemisorbed as a carbonyl with the removal of two free valencies.

In all cases, the variation of bonding strength of chemisorbed H_2, Cl_2, and O_2 species is very evident, since about 50% of the measured desorption occurred between 200 and 600°C and the remaining desorption occurred from 600 to 950°C for Cl_2, from 300 to 450 to 950°C for O_2, and from 500 to 700 to 950°C for H_2. The original conversion-equilibration rates were completely restored by outgassing at 950°C.

For H_2 treatment, the values of paramagnetic rate parameters a and φ observed at degassing temperatures below the point at which much desorption of H_2 occurred were associated with high values of b, indicating a low coverage θ at active sites. Since b is determined from tests under set conditions with P_T as the only variable and is not, therefore, affected by the number of sites available, this is evidence that the specific rates of adsorption-desorption are affected by the poisoning species in addition to the area or number of active sites available. The low value of θ would indicate a higher specific rate of desorption, implying a weaker bonding of the active chemisorbed species. Since activated chemisorption of hydrogen would be expected to poison the stronger bonding sites preferentially, the unaffected active sites might be expected to be of a weaker bonding nature than the original surface.

Partially covering the surface by treatment with H_2 at 900°C did not give exactly the same relations between amount remaining adsorbed after partial degassing and rates, presumably because the surface composition as a function of degree of bonding was not independent of the path taken to reach a given surface coverage.

B. Graphon

The results for Graphon show many similarities to the diamond results, but also some striking differences. The o-p and $H_2/D_2/HD$ rates are no longer close, and the paramagnetic and chemical mechanisms are of comparable magnitude. The values of b for the chemical rates are no longer small, indicating a fractional coverage of active sites, even at 77 K. The values of b for the o-p rate, which are effective means of the paramagnetic and chemical mechanisms, are low at 77 K, indicating $\theta \to 1$ for the paramagnetic mechanism.

Because higher reaction temperatures were investigated, the increase in rate with temperature for the second, higher-temperature portion of the Arrhenius plot (which was predicted in Sec. III) is now experimentally confirmed (see Fig. 21). The activation energy and preexponential factor of ω in this region are 13.6 kcal/mole and $(4.2)(10^{15})$ molecules/cm^2 · sec. This clearly demonstrates a new chemical mechanism (although the same forms of rate and kinetic equations still apply) involving a transition state of high activation energy but lower activation entropy.

Unlike diamond, high-temperature poisoning by oxygen destroys the low-temperature paramagnetic conversion as well as the chemical conversion on the Graphon (Fig. 22). However, if the Graphon is partially burned out, oxygen poisoned, and retested, there is an initial paramagnetic rate before oxygen desorption, and the results become more comparable to those of diamond. The paramagnetic rate is somewhat enhanced by partial removal of oxygen as CO_2 and possibly water. Carbon dioxide continued to be desorbed up to an outgassing temperature of 650°C, and desorption of CO_2 is considered to create paramagnetic sites. Harker and co-workers [70] studied the reaction of cellulose carbons with oxygen by ESR. They found a maximum in the number of unpaired electrons when it was plotted against heat treatment temperature. They have

suggested that this maximum is due to release of CO_2, since release of CO_2 also has a maximum at the same heat treatment temperature near 600°C. In this case, however, release of CO_2 is not likely to be responsible for a maximum, since the cumulative amount of CO_2 desorbed is less than one-tenth of the cumulative CO desorbed upon outgassing at 600°C. The desorbed CO_2 could be coming from lactone or anhydride structures [82], and since these groups are less common on the surface, the free valencies produced on the surface would be isolated with little possibility of interaction. The probability of rehybridization to delocalize these electrons would be low due to the remaining chemisorbed oxygen which would place restraints on rehybridization.

Turkevich and Laroche [31], studying a graded set of sugar charcoals prepared at 300°C and then heat treated in vacuo, found maxima at 605°C in plots of the rate of conversion at 77 K and the number of unpaired electrons, as determined by ESR, against heat treatment temperature. The gradual continuous increase in the rate of equilibration at 50°C above a heat treatment temperature of 605°C was also observed and attributed to an increase in the interaction between electrons. But this work can be criticized since the cause of the maximum is not clear; it could be due both to the removal of oxygen on the surface and to some reorganization of the carbon bulk resulting from an increase in the heat treatment temperature.

Seanor [68] studied the conversion at 90 K on three different charcoals and found behavior similar to that observed by Turkevich and Laroche [31]. In the case of Seanor's work, however, it is possible to unequivocally associate the maxima in both the rate of conversion and number of spins versus temperature of heating in vacuum with oxygen chemisorbed on the surface of the carbons, since his samples were previously treated at 1000°C. Seanor regarded this as explicable only if small quantities of oxygen can form quinone structures, which place restraints on the amount of delocalization allowed via the π bonding.

The maximum rates of conversion calculated in terms of active surface area and BET area are given in Table 11. The rate expressed per unit of active area is almost constant [about 2.5×10^{13} molecules/cm^2(ASA) · sec] for all samples. This indicates that the active surface area (edge carbon atoms) for oxygen chemisorption is responsible for paramagnetic conversion. However, after

TABLE 11

Variation of the Maximum Conversion Rate with Burn-Off of Graphon

Graphon (% B.O.)	10^{12} molecules/ cm^2 (BET) · sec	10^{13} molecules/ cm^2 (ASA) · sec
0.0	0.07	2.25
3.7	0.53	2.93
15.9	1.02	2.51
24.9	1.20	2.51
37.9	1.30	2.50
70.5	1.47	2.52
15.9 (heat treated)	0.50	2.95

outgassing at 600°C, about 30% of chemisorbed oxygen atoms remain on the surface. Further removal of surface oxygen complexes causes a decrease in the rate of paramagnetic conversion while the rate of equilibration increases. According to the work on decomposition of surface oxygen complex on Graphon by Bansal et al. [83], who have proposed that chemisorption of oxygen takes place on different discrete configurations of sites on the carbon surface [59, 60], the oxygen is desorbed (as CO and CO_2) from different sites. They have suggested that upon outgassing up to 600°C, the oxygen is desorbed primarily from sites having a carbon-carbon spacing of 2.8 Å in the $(11\bar{2}0)$ surface, with a small amount of oxygen coming from sites having carbon-carbon spacings of 3.62 and 3.35 Å. The oxygen desorbed during outgassing at temperatures higher than 600°C could be coming from sites having spacings of 2.46 Å in the $(10\bar{1}0)$ surface and 1.42 Å in the $(11\bar{2}0)$ surface. This would lead us to suggest that spins which cause the conversion were localized on oxygen species chemisorbed on the edge carbons in the $(10\bar{1}0)$ surface, probably in the form of paramagnetic O^- ions, and at free valencies at edge carbons in the $(11\bar{2}0)$ surface. Coulson [51] has suggested that the bond of edge carbon atoms in the $(11\bar{2}0)$ surface may acquire a partly triple-bond character and saturate the free valencies. However, recent theoretical calculations by Bennett et al. [52] indicate that the edge arrangement with saturated free valencies in the $(11\bar{2}0)$ surface is energetically unfavorable.

When chemisorbed oxygen on the edge carbon atoms in the $(10\bar{1}0)$ surface desorbs, free valencies on the edge carbon atoms are likely to interact with each other, and rehybridization into an s^2p^2 configuration, as proposed by Coulson, is probable. These sites no longer cause the conversion through a paramagnetic mechanism, but may cause the conversion and equilibration through the Schwab-Killmann mechanism because of their favorable geometry and strong interaction between free valencies. Michael [71] found in his studies on the effect that oxygen complexes on Graphon have upon ESR that the number of unpaired electrons decreases with increasing outgassing temperatures above 600°C and that this decrease is accompanied by an increase in line width, indicating an increase in the interaction between electrons. Turkevich and Laroche [31] found that the catalytic activity of the carbon for the equilibration increased monotonically with increasing heat treatment temperature above 600°C and that the ESR of these carbons showed an increase in line width. They suggested that the active sites for the equilibration are associated with the presence of a domain of interacting electrons.

The rate of equilibration on samples outgassed at 950°C and the number of oxygen atoms desorbed during outgassing after the rate of conversion passed through the maximum are shown in Table 12. The rate is linearly proportional to the number of desorbed atoms. This is consistent with the conclusion that removal of chemisorbed oxygen at the edge carbon atoms in the $(10\bar{1}0)$ surface creates active sites for the equilibration.

Singer et al. [84] found that chemisorption of oxygen on sucrose char at 450°C decreases the spin-lattice relaxation time by 10^2, whereas this investigation shows that the rate of paramagnetic conversion increases by chemisorption of oxygen. As discussed before, Leffler [15] has predicted that paramagnetic ions of longer spin-lattice relaxation time should be a better catalyst for paramagnetic conversion than ions of shorter relaxation time. The results of this study, which are adequately explained by Wigner's original theory extended to cover conversion in an adsorbed layer, do not support this prediction.

A most striking feature of the results for Graphon is that the rate expressions all fit the same simple rate expressions, whether the chemical mechanism or paramagnetic mechanism was dominant, or whether the low-temperature or

TABLE 12

Equilibration Rate at 77 K and Desorption of Oxygen from Graphon Between 600 and 950°C

Graphon (% B.O.)	10^{11} molecules/ $cm^2 \cdot sec$	Oxygen desorbed (10^{13} atoms/cm^2)
0.0	0.06	0.09
3.7	1.10	0.70
15.9	2.33	1.55
24.9	2.38	1.65
37.9	2.48	1.60
70.5	2.30	1.50

high-temperature regions were considered, or whether poisoning species did or did not exist on the surface.

This feature plus the comments made above concerning the role of dissociated hydrogen species suggests that the chemical mechanism should be similar in structure to the paramagnetic mechanism, involving reaction of adjacent adsorbed hydrogen molecules. This is the Schwab-Killman mechanism. However, a logical problem exists for this mechanism in that the low-temperature chemical mechanism has a low activation energy.

The poisoning mechanism does not seem to be solely related to blocking of mobility on the surface, since poisoning was very evident even at appreciable desorption of poisoning molecules. Since the first molecules to desorb are from weakly bonding sites, these are the sites expected to be effective in surface mobility. It seems more reasonable to explain poisoning via blocking of the active sites. A major logical problem, however, is that the active sites opened on desorption appear to behave similarly to each other irrespective of the increment of temperature necessary to open them up. Thus, the temperature coefficients of the degassed, unpoisoned surface are consistent with two types of site for the chemical mechanism rather than a whole range of sites of varying bonding.

The sites involved must make up a very small fraction of the total surface. The low preexponential coefficients, combined with the above statement on the role of surface mobility, would suggest an immobile mechanism, with a low probability of a surface structure with just the right features to promote a low activation energy exchange of atoms between adjacent adsorbed molecules.

ACKNOWLEDGMENT

We appreciate Professor H. P. Boehm supplying the diamond powder used in this study and also supplying the diamond samples on which chlorine, oxygen, and hydrogen had been chemisorbed.

REFERENCES

1. A. Farkas, Orthohydrogen, Parahydrogen and Heavy Hydrogen, Cambridge Univ. Press, London, 1935.
2. D. D. Eley, Advances in Catalysis, Vol. 1, (W. G. Frankenburg, V. I. Komarewsky, and E. K. Rideal, eds.). Academic Press, New York, 1948, p. 157.
3. B. M. W. Trapnell, Catalysis, Vol. 3, (P. H. Emmett, ed.), Reinhold, New York, 1955, p. 1.
4. D. Brennan, Recent Progress in Surface Science, Vol. 2, (J. F. Danielli K. G. A. Pankhurst, and A. C. Riddiford, eds.), Academic Press, New York, 1964, p. 57.
5. G. E. Schmauch and A. H. Singleton, Ind. Eng. Chem., 56, 20 (1964).
6. K. F. Bonhoeffer and P. Harteck, Z. Physik. Chem. Abt. B, 4, 113 (1929).
7. H. S. Taylor, J. Amer. Chem. Soc., 53, 578 (1931).
8. K. W. Rummel, Z. Physik. Chem. Abt. A, 167, 221 (1933).
9. H. S. Taylor and H. Diamond, J. Amer. Chem. Soc., 55, 2613 (1933).
10. D. D. Eley, Trans. Faraday Soc., 36, 500 (1940).
11. L. Farkas and Y. L. Sandler, J. Chem. Phys., 8, 248 (1940).
12. L. Farkas and H. Sachsse, Z. Physik. Chem. Abt. B, 23, 1 (1933).
13. E. Wigner, Z. Physik. Chem. Abt. B, 23, 28 (1933).
14. F. Kalckar and E. Teller, Proc. Roy. Soc. Ser. A, 150, 520 (1935).
15. A. J. Leffler, J. Chem. Phys., 43, 4410 (1965).
16. H. S. Taylor and A. Sherman, Trans. Faraday Soc., 28, 247 (1932).
17. K. F. Bonhoeffer and A. Farkas, Z. Physik. Chem. Abt. B, 12, 231 (1931).
18. K. F. Bonhoeffer and A. Farkas, Trans. Faraday Soc., 28, 242, 561 (1932).

19. E. K. Rideal, Proc. Camb. Phil. Soc., 35, 130 (1939).

20. D. D. Eley, Trans. Faraday Soc., 44, 216 (1948).

21. G. M. Schwab and E. Killmann, Actes Congr. Int. Catal. 2nd, 1, 1047 (1960).

22. D. D. Eley and D. Shooter, J. Catal., 2, 259 (1963).

23. J. J. F. Scholter and J. A. Konvalinka, J. Catal., 5, 1 (1966).

24. W. R. Alcorn and T. K. Sherwood, J. Catal., 6, 288 (1966).

25. S. Ohno and I. Yasumori, Bull. Chem. Soc. Jap., 41, 2227 (1968).

26. K. F. Bonhoeffer, A. Farkas, and K. W. Rummel, Z. Physik. Chem. Abt. B, 21, 225 (1933).

27. R. Juza, J. Langheim, and H. Hahn, Angew. Chem., 51, 354 (1938).

28. A. J. Gould, W. Bleakney, and H. S. Taylor, J. Chem. Phys., 2, 362 (1934).

29. A. Farkas and L. Farkas, Nature, 132, 894 (1933).

30. A. Farkas and L. Farkas, Proc. Roy. Soc. Ser. A, 144, 16, 467 (1934).

31. J. Turkevich and J. Laroche, Z. Physik. Chem., 15, 399 (1958).

32. M. J. Rossiter, R. N. Smith, and J. R. Ludden, J. Phys. Chem., 67, 2541 (1963).

33. J. Koutecky and M. Tomasek, Phys. Rev., 120, 1212 (1960).

34. J. Koutecky, Angew. Chem., 76, 365 (1964).

35. D. Pugh, Phys. Rev. Lett., 12, 390 (1964).

36. R. E. Schlier and H. E. Farnsworth, Semiconductor Surface Physics, Univ. of Pennsylvania Press, Philadelphia, 1957, p. 13.

37. H. E. Farnsworth, R. E. Schlier, J. H. George, and R. M. Burger, J. Appl. Phys., 29, 1150 (1958).

38. H. E. Farnsworth and J. Marsh, Bull. Amer. Phys. Soc., 5, 349 (1960).

39. M. Green and R. Seiwatz, J. Chem. Phys., 37, 459 (1962).

40. J. Marsh and H. E. Farnsworth, Surface Sci., 1, 3 (1964).

41. J. J. Lander and J. Morrison, Surface Sci., 4, 241 (1966).

42. H. P. Boehm, E. Diehl, W. Heck, and R. Sappok, Angew. Chem., 76, 742 (1964).

43. E. Storfer, Z. Elektrochem., 41, 868 (1935).

44. E. Storfer, Trans. Faraday Soc., 34, 639 (1938).

45. R. W. Barrer, J. Chem. Soc., 1256 (1936).

46. R. M. Barrer, J. Chem. Soc., 1261 (1936).

47. H. P. Boehm, Angew. Chem., 78, 617 (1966).

48. R. Sappok and H. P. Boehm, Carbon, 6, 283 (1968).

49. R. Sappok and H. P. Boehm, Carbon, 6, 573 (1968).

50. L. Pauling, The Nature of the Chemical Bond, Cornell Univ. Press, New York, 1960.

51. C. A. Coulson, Proceedings of the Fourth Carbon Conference, Pergamon Press, Oxford, 1960, p. 215.

52. A. J. Bennett, B. McCarroll, and R. P. Messmer, Phys. Rev. B, 3, 1397 (1971).

53. R. H. Savage and C. Brown, J. Amer. Chem. Soc., 70, 2362 (1948).

54. R. H. Savage, Ann. N.Y. Acad. Sci., 53, 862 (1951).

55. W. R. Smith and M. H. Polley, J. Phys. Chem., 60, 689 (1956).

56. L. Bonnetain, X. Duval, and M. Letort, Proceedings of Fourth Carbon Conference, Pergamon Press, Oxford, 1960, p. 107.

57. N. R. Laine, F. J. Vastola, and P. L. Walker, Jr., Proceedings of the Fifth Carbon Conference, Vol. 2, Pergamon Press, Oxford, 1963, p. 211.

58. N. R. Laine, F. J. Vastola, and P. L. Walker, Jr., J. Phys. Chem., 67, 2030 (1963).

59. P. L. Walker, Jr., R. C. Bansal, and F. J. Vastola, The Structure and Chemistry of Solid Surfaces, Wiley, New York, 1969, p. 81.

60. R. C. Bansal, F. J. Vastola, and P. L. Walker, Jr., J. Colloid Interface Sci., 32, 187 (1970).

61. R. C. Bansal, F. J. Vastola, and P. L. Walker, Jr., Carbon, 9, 185 (1971).

62. S. Mrozowski, Carbon, 3, 305 (1965).

63. G. Wagoner, Proceedings of the Fourth Carbon Conference, Pergamon Press, Oxford, 1960, p. 197.

64. G. Wagoner, Phys. Rev., 118, 647 (1960).

65. K. Antonowicz, Carbon, 1, 111 (1967).

66. G. M. Arnold, Carbon, 5, 33 (1967).

67. S. Mrozowski and J. F. Andrew, Proceedings of the Fourth Carbon Conference, Pergamon Press, Oxford, 1960, p. 207.

68. D. A. Seanor, Ph.D. thesis, Univ. of Bristol, England, 1961.

69. D. E. G. Austen, D. J. E. Ingram, and J. G. Tapley, Trans. Faraday Soc., 54, 400 (1958).

70. H. Harker, J. T. Gallagher, and A. Parker, Carbon, 4, 401 (1966).

71. G. C. Michael, Ph.D. thesis, The Pennsylvania State Univ., University Park, 1969.

71a. Y. Ishikawa, Ph.D. thesis, The Pennsylvania State University, University Park, Pennsylvania, 1971.

72. H. W. Wolley, R. B. Scott, and F. G. Brickwedde, J. Res. Nat. Bur. Stand., 41, 379 (1948).

73. J. L. Bolland and H. W. Melville, Trans. Faraday Soc., 33, 1316 (1937).

74. D. R. Ashmead, D. D. Eley, and R. Rudham, Trans. Faraday Soc., 59, 207 (1963).

75. G. A. Wolff and J. D. Broader, Acta Crystallogr., 12, 313 (1959).

76. F. H. Van Cauwelaert and W. H. Hall, Trans. Faraday Soc., 66, 454 (1970).

77. J. H. de Boer, The Dynamic Character of Adsorption, Oxford Univ. Press, London, 1968.

78. P. Handler, Semiconductor Surface Physics, Univ. of Pennsylvania Press, Philadelphia, 1957, p. 23.

79. E. W. Neuman, J. Chem. Phys., 2, 31 (1934).

80. Y. Shigehara and A. Ozaki, J. Catal., 10, 183 (1968).

81. D. S. Chapin, C. D. Park, and M. L. Corrin, J. Phys. Chem., 64, 1073 (1960).

82. R. N. Smith, D. A. Young, and R. A. Smith, Trans. Faraday Soc., 62, 2280 (1966).

83. R. C. Bansal, F. J. Vastola, and P. L. Walker, Jr., Carbon, 8, 443 (1970).

84. L. S. Singer, W. J. Spry, and W. H. Smith, Proceedings of the Third Carbon Conference, Pergamon Press, Oxford, 1959, p. 121.